UNIVERSITY OF

MARYLAND

Technical Note BN-652 April 1970

MEASURED OPTICAL ABSORPTION COEFFICIENTS FOR URANIUM PLASMAS

by

M. H. Miller, T. D. Wilkerson and R. Roig

THE INSTITUTE FOR FLUID DYNAMICS

and

APPLIED MATHEMATICS

NASA CR-72661

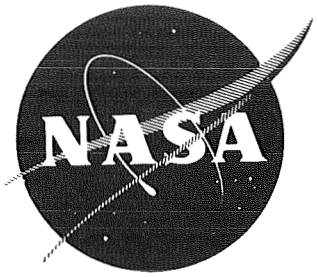

Technical Note BN-652 April 1970

MEASURED OPTICAL ABSORPTION COEFFICIENTS FOR URANIUM PLASMAS

by

M. H. Miller, T. D. Wilkerson and R. Roig

*Research supported by NASA Grant NGR-21-002-167 (monitor R. W. Patch, Lewis Research Center) and by the University of Maryland through the Regents, the Minta Martin Fund and the Department of Electrical Engineering and the Institute for Fluid Dynamics and Applied Mathematics.

NASA CR-72661

MEASURED OPTICAL ABSORPTION COEFFICIENTS FOR URANIUM PLASMAS

by

M. H. Miller, T. D. Wilkerson and R. Roig

prepared for

NATIONAL AERONAUTICS AND SPACE ADMINISTRATION

April 1970

Grant NGR-21-002-167

Technical Monitor
NASA Lewis Research Center
Cleveland, Ohio
Nuclear Systems Division
R. W. Patch

Institute for Fluid Dynamics and Applied Mathematics
University of Maryland
College Park, Maryland

ABSTRACT

Absolute emissivities of uranium plasmas (3000-8800 Å) were measured using a gas-driven shock tube. Temperatures (7500-12,000 K) and uranium partial pressures (1/30-1/3 atmos.) approach those anticipated at the hydrogen-uranium interface of proposed gas-core nuclear reactors. At these conditions, uranium (UI, UII, UIII) is essentially the only spectroscopically active constituent of shock tube test gases composed of 0.2-2.0% UF_6 in neon. Absolute emissivities at 5000 Å are measured photoelectrically both in emission and in absorption. The variation of emissivity with wavelength was obtained from time-resolved photographic recordings. Measured visible emissivities are 2-5 times smaller than theoretical predictions, depending on the plasma's state. Emissivity (and opacity) decrease with increasing temperature slightly more rapidly than theory predicts. The dependence of emissivity on uranium density is an order of magnitude greater than expected theoretically. The data suggest that the continuum is more important than previously supposed. Between 4000-8800 Å, emissivity varies with wavelength in essentially the predicted way; however, a predicted surge in ultraviolet (3000-4000 Å) emissivities was not observed.

MEASURED OPTICAL ABSORPTION COEFFICIENTS FOR URANIUM PLASMAS

ABSTRACT ---------- i

I. INTRODUCTION ---------- 1

II. METHOD: Principles ---------- 3

A. Definitions and Review of Radiative Transfer ---------- 3

B. Determination of Optical Depth and Temperature via Emission and Absorption Measurements ---------- 4

C. Complications due to Limited Spectral Resolution ---------- 6

III. EXPERIMENTAL ---------- 9

A. Apparatus ---------- 9

B. Test Gas Preparation ---------- 14

C. Plasma Pressure Measurements ---------- 15

D. Plasma Temperature Measurements ---------- 15

E. Electron Density Measurements ---------- 21

F. Intensity and Emissivity Measurements ---------- 21

IV. RESULTS AND DISCUSSION ---------- 29

A. Absolute Mass Absorption of Uranium Plasma ---------- 29

B. Variation of Emissivity with Wavelength ---------- 35

C. Work in Progress ---------- 40

V. CONCLUSIONS ---------- 43

REFERENCES ---------- 45

I. Introduction

The feasibility of proposed gaseous core nuclear reactors[1] depends critically upon the optical properties of uranium gas at temperatures of order 10,000 - 50,000°K. Radiative transfer out of this hot gas simultaneously offers an efficient means of extracting the available energy, and presents basic problems with respect to confinement pressure balance and system weight. A sample of uranium gas at a given temperature and pressure will emit a certain amount of energy, distributed over wavelength in a complicated way. Both this total flux and its spectral distribution must be known in order to obtain optimal coupling between the core and working fluid of the reactor.[2,3,4] Good coupling, in turn, is necessary if advanced concept rocket motors[1], such as the one shown schematically in Figure 1, are to attain desirable levels of thrust and specific impulse, or if MHD power generators[5] are to become economically competitive. Moreover, the rapidly flowing working fluid, usually seeded high pressure hydrogen, must effectively absorb all the radiation, so that the reactor walls will not evaporate under anticipated heat loads of order 100 kW/cm^2.

Optical coefficients of uranium plasmas have been calculated for wide ranges of pressure and temperature. Because of the extremely complex atomic structure of uranium[6,7], the requisite theoretical models involve more than the usual assumptions.[8,9] Opacities predicted by this model have been compared with a numerical synthesis of experimental results from a free-burning arc.[8] The theory appears to be transformable into the one available experimental result, by means of a parameter adjustment; how general this may be is not known. Because the arc (T = 5100°K) excites in fact relatively few of the lines expected at fissioning core conditions, statistical assumptions in the model are likely to be less applicable then for plasmas at higher temperature. Moreover,

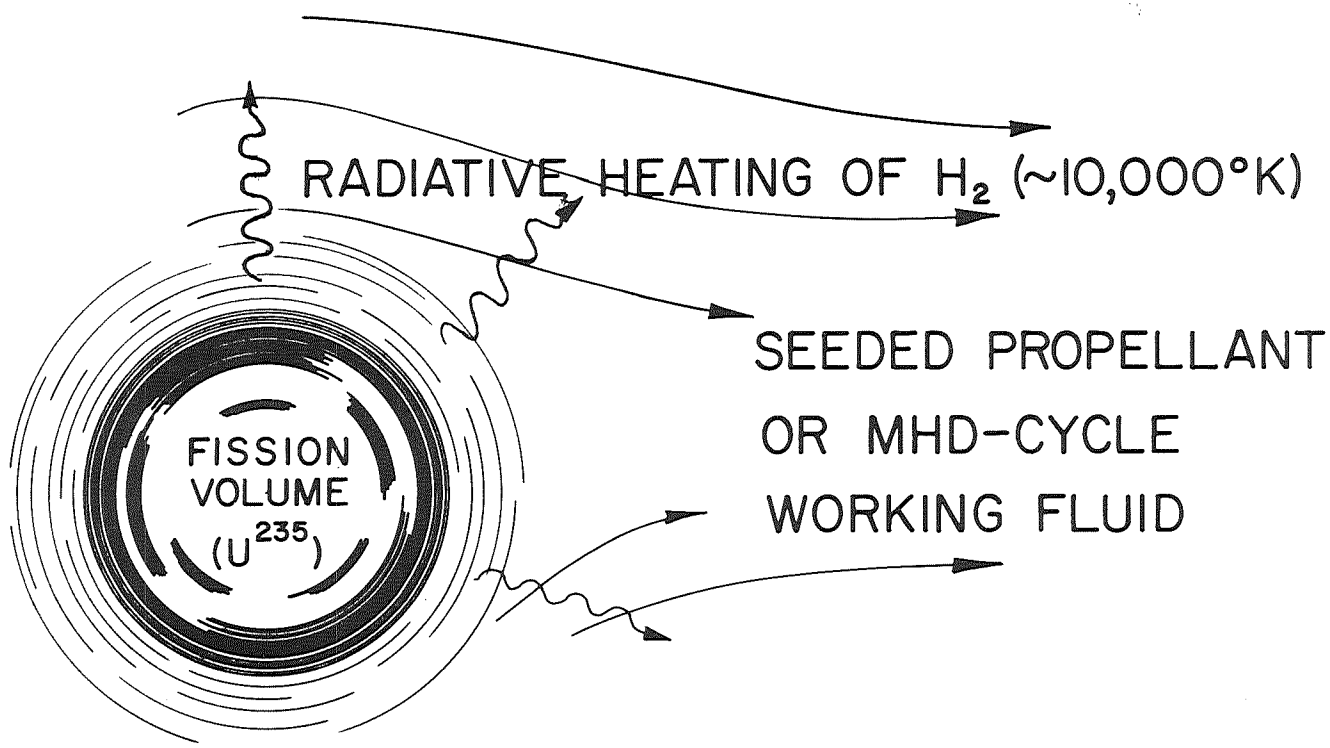

Figure 1. Principle of the gas-core fission reactor.

electron-ion densities in the arc are generally too small to provide much data on the recombination spectra of uranium

The current experiment is intended, in part, to test the reliability of the sophisticated predictions that have been made. The experimental conditions cover a restricted portion (8,000 - 12,000°K, 0.03 - 0.30 atmos.) of the pressure-temperature domains (8,000 - 50,000°K, 0.01 - 500 atmos.) that must be considered for an overall picture of gaseous-core operation. Testing over even a limited range may help to identify the good and bad features of the theoretical model. Insofar as our shock tube plasmas do approach the temperatures and uranium partial pressures anticipated at the hydrogen-uranium interface[1] of open-cycle reactors, the present data should directly benefit calculations of radiative transfer in this important region.

The gas driven shock tube is well suited to absolute emissivity studies.[10,16] The relatively large (1-2 liter), stationary plasma generated behind reflected shocks persists in a steady state for periods of 50-200 μsec. This duration is adequate to establish local thermodynamic equilibrium (LTE) and provide ample test time for spectroscopic sampling techniques. It is too short, however, to permit plasma constituents of different masses to demix. In consequence, optical properties (emissivity or optical depth) can be directly related to the number and type of emitters in a spectroscopic line of sight. With zoned light sources such as the DC arc,[17,18] the possibility of demixing along strong thermal gradients does not permit such a simple correlation.

II. Method: Principles

A. Definitions and Review of Radiative Transfer

The specific intensity of light emerging normally from a homogeneous slab of plasma is[19-22]

$$I = I_o e^{-\tau} + B(T)\ (1 - e^{-\tau}) \qquad (1)$$

where τ is the optical depth (at a given wavelength), $B(T)$ is the Planck function (Black body intensity) at this wavelength, and I_o is the specific intensity of light entering the opposite side of the plasma. The absorptivity K for this wavelength is $K = \tau/\ell$, where ℓ is the thickness of the plasma.

Optical depth is commonly converted into some intensive coefficient which is less geometry dependent, or less dependent on other incidental factors. For a multicomponent gas, a convenient parameter is the mass-absorption coefficient K_M which for any source, when multiplied by the number of grams/cm^2 in the line of sight, will give the dimensionless optical depth and all derivative quantities. Letting $\rho(U)$ be the mass density of uranium,

$$K_M = K/\rho(U) \ ;$$

$$\left[\frac{cm^2}{gm}\right] = \left[\frac{1}{cm}\right] \Big/ \left[\frac{gm}{cm^3}\right]$$

The local Plank means of τ, K, and K_M are defined as linear averages of these quantities over the resolved bandwidth.(8)

B. Determination of Optical Depth and Temperature via Emission and Absorption Measurements

Optical depths of shock tube plasmas are measured by two independent techniques. The emission technique utilizes a photomultiplier that has been calibrated against the known (absolute) spectral irradiance of a regulated carbon arc.(23) This is used to record the plasma intensity I emitted in some bandpass. If the plasma is not backlighted ($I_o = 0$), and a measured plasma temperature is available for computation of $B(T)$, then the optical depth is obtained via equation (1)

$$\tau = - \ln \left\{1 - \frac{I}{B(T)}\right\} \ ;$$

i.e., the optical depth at every wavelength follows directly from the measured intensity I at that wavelength and the known temperature of the gas in the shock tube.

Optical depth can also be measured by using a short duration flashlamp[24-26] whose locally grey emission at any instant can be characterized by an effective brightness $B(T(t))$. The lamp is discharged at an appropriate time to backlight the shock tube plasma. For some portion of its discharge (half-duration $\sim$ 3 μsec), the lamp's brightness exceeds the black body intensity of the shock tube. A detector which records a shock tube intensity of $B(T)[1 - e^{-\tau}]$ before the onset of the flashlamp, will in the course of the discharge, record $B(T)[1 - e^{-\tau}] + B(T(t))e^{-\tau}$. If the flashlamp is subsequently fired in the absence of an attenuating shock tube plasma, the recorded signal will cross over the previously (shock tube + flashlamp) recorded signal at two points (reversal points*). The intensity corresponding to these crossing points is described by[26]

$$B(T(t)) = B(T(t))e^{-\tau} + B(T)\{1 - e^{-\tau}\} \qquad (2)$$

or equivalently, by

$$T(t) = T \quad .$$

That is, the intensity at the reversal points is the black body intensity for the shock tube plasma. The optical depth can therefore be obtained directly from the ratio of two signals sequentially recorded on the same photomultiplier:

$$\frac{\text{shock tube intensity prior to flashlamp}}{\text{reversal intensity}} = \frac{B(T)\{1 - e^{-\tau}\}}{B(T)} = (1 - e^{-\tau}) \quad . \qquad (3)$$

---

* The name derives from the vanishing of the spectral features and the reversal from an emission (absorption) spectrum to an absorption (emission) spectrum at that time, the choice depending on increasing (decreasing) specific intensity of the background illumination.

An obvious advantage of this technique is that no absolute intensity calibration is required if an emissivity is the only desired result. If the detector is calibrated absolutely, the reversal intensity (Planck function) can be solved to find the plasma temperature.

C. Complications Due to Limited Resolution

Optical depth is a concept strictly applicable to infinitesimal wavelength intervals.[19-22,27] Spectrographs, however, collect light through slits of finite width, thereby impressing some bandpass $\Delta\lambda$ upon the data. If the spectral features of interest are considerably broader than $\Delta\lambda$, convolution integrals can be used to unfold the instrumental profile.[28] This is not feasible in the present study because uranium line widths are much narrower than our best resolution. Perforce, we measure

$$(1 - e^{-\tau})_{avg}\Delta\lambda \equiv \int_{-\Delta\lambda/2}^{\Delta\lambda/2} [1 - e^{-\tau}]d\lambda \qquad (3)$$

and consequently

$$\tau_{avg}\Delta\lambda \leq \int_{-\Delta\lambda/2}^{\Delta\lambda/2} \tau \, d\tau \ .$$

The equality holds only in the limit $\tau \to 0$. The extent of the inequality depends on both the mean value of τ and is variation with wavelength in the interval $\Delta\lambda$. There would be little or no significant error for a continuum, while a spectrum composed of alternately spaced gaps and strong, narrow lines could present a serious problem.

In the absence of any reliable estimates for the Stark-effect[29-31] broadening of UI and UII lines, it will be assumed that line widths are due exclusively to thermal broadening; this is the worst possible case from the standpoint of converting emissivity data to opacities. In this assumption line profiles have Gaussian shape, and the (full) Doppler halfwidths of all lines will be ≈ 0.03 Å. The instrumental profile at the wavelength of optimal focus has a full width of 0.20 Å and a shape which rather closely approaches pure Gaussian. The spectrograph slit therefore redistributes the line's energy over a six-times wider wavelength interval, while reducing the apparent peak brightness, $B(T)\ (1 - e^{-\tau^*_{max}})$, to 1/6 of the true value $B(T)\ (1 - e^{-\tau_{max}})$. In Figure 2 we indicate the loss of recorded (integrated) line intensity due to radiative trapping, $\int [1 - e^{-\tau}]\tau^{-1} d\lambda$, as a function of the apparent optical depth τ^* at the line center. While this loss occurs regardless of the instrument profile, it could be strictly accounted for with the aid of temperature and absolute intensity data if the profiles were well resolved. Because the total width of two convoluted Gaussian profiles is the RMS sum of the individual widths[28], a strong uranium line could get very bright indeed ($\tau_{max} \rightarrow 6$) before apparent broadening due to saturation would be detectable. In a typical experiment (1/2% UF_6 in neon; 10,500°K) the brighter uranium lines (mostly UII) attain τ^*_{max} values of 0.2 - 0.4, so that by the pessimestic analysis of Figure 2 we could underestimate the lines' overall contribution to the opacity by a factor of 4 - 8. However, the most prominent lines are not very densely spaced, occurring on the average with intervals of 5 Å in the violet, 10 Å in the green and 20 Å in the red. Considering the 0.04 Å width of these lines, together with the fact that apparent continuum emissivities at the assumed plasma conditions range between 0.05 - 0.20, our inability to resolve the lines may cause measured

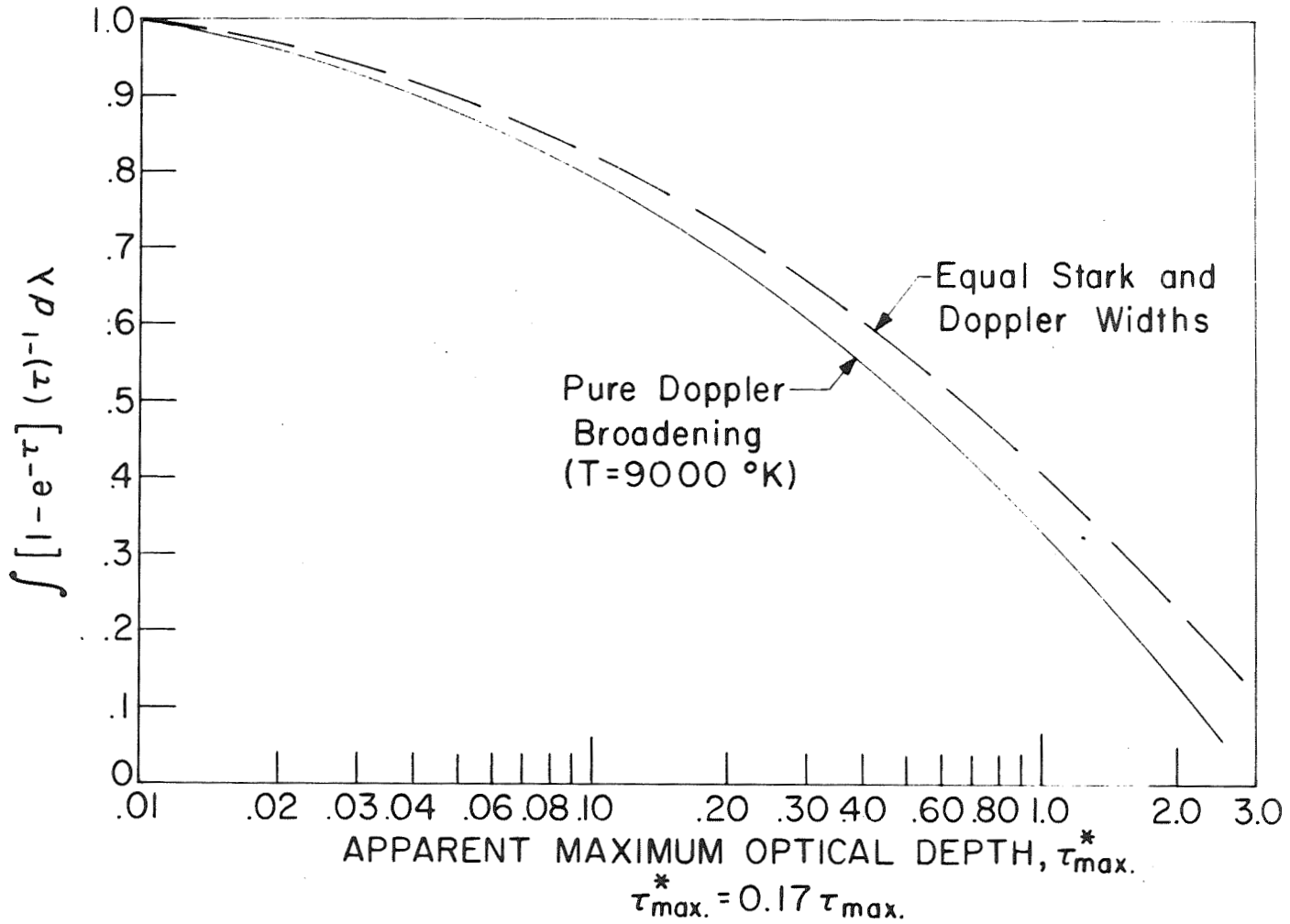

Figure 2. Dependence of uranium line strengths, recorded with insufficient resolution, upon measured (apparent) optical depths at the line centers, τ^*_{max}. When instrument widths are $(0.17)^{-1}$ times the line halfwidths, only the fraction $\int[1-e^{-\tau}]/\tau d\lambda$ of the line's total energy is recorded. Rigorous corrections for radiative trapping could be made if relevant Stark broadening parameters were available.

local opacities to err by at most 30% (in the violet). At higher, and lower, wavelengths, the error will be smaller, particularly for shocks where uranium concentrations enhance the continuous spectrum.

III. Experimental

A. Apparatus

Our conventional shock tube has a rectangular cross-section (6.7 × 9.3 cm) and an expansion section length of 315 cm . Interior surfaces are chromium plated mild steel. Normally, 40-75 atmos. of cold hydrogen is used to drive the shocks. By controlling the depth of an X-shaped relief, breaking pressure of the soft aluminum diaphragms, can be regulated to within ±3% .[32] A liquid nitrogen-baffled 4" diffusion pump used in conjunction with dry-nitrogen backfilling and special high conductance values,[32] evacuates the shock tube to base pressures of $1\text{-}5 \times 10^{-5}$ torr at a cycling rate of one experiment per hour.

White-light, streak (x - t) photographs taken with a rotating drum camera showed incident and reflected shocks to be well formed and the optically thin plasmas behind them to be free from strong vortices or diagonal waves. Sometimes weak disturbances could be detected in the nearly stationary 1 - 2 liter spectroscopic source region behind first reflected shocks. These perturbations to plasma homogeneity could not be made to repeat in either strength or time behavior, so while they probably contribute somewhat to the scatter in spectroscopic data,[32] we feel that there is no way they can introduce systematic bias. A variety of spectroscopic tests, described elsewhere,[32-35] failed to disclose any of the more common forms of bias.

Present instrumentation is shown schematically in Figure 3. The two versions used for the work reported here differ from the illustration in that

(i) initially the spectrograph (c) employed a rotating drum camera rather than a fast shutter, and spectrograph (d) had not yet been obtained,

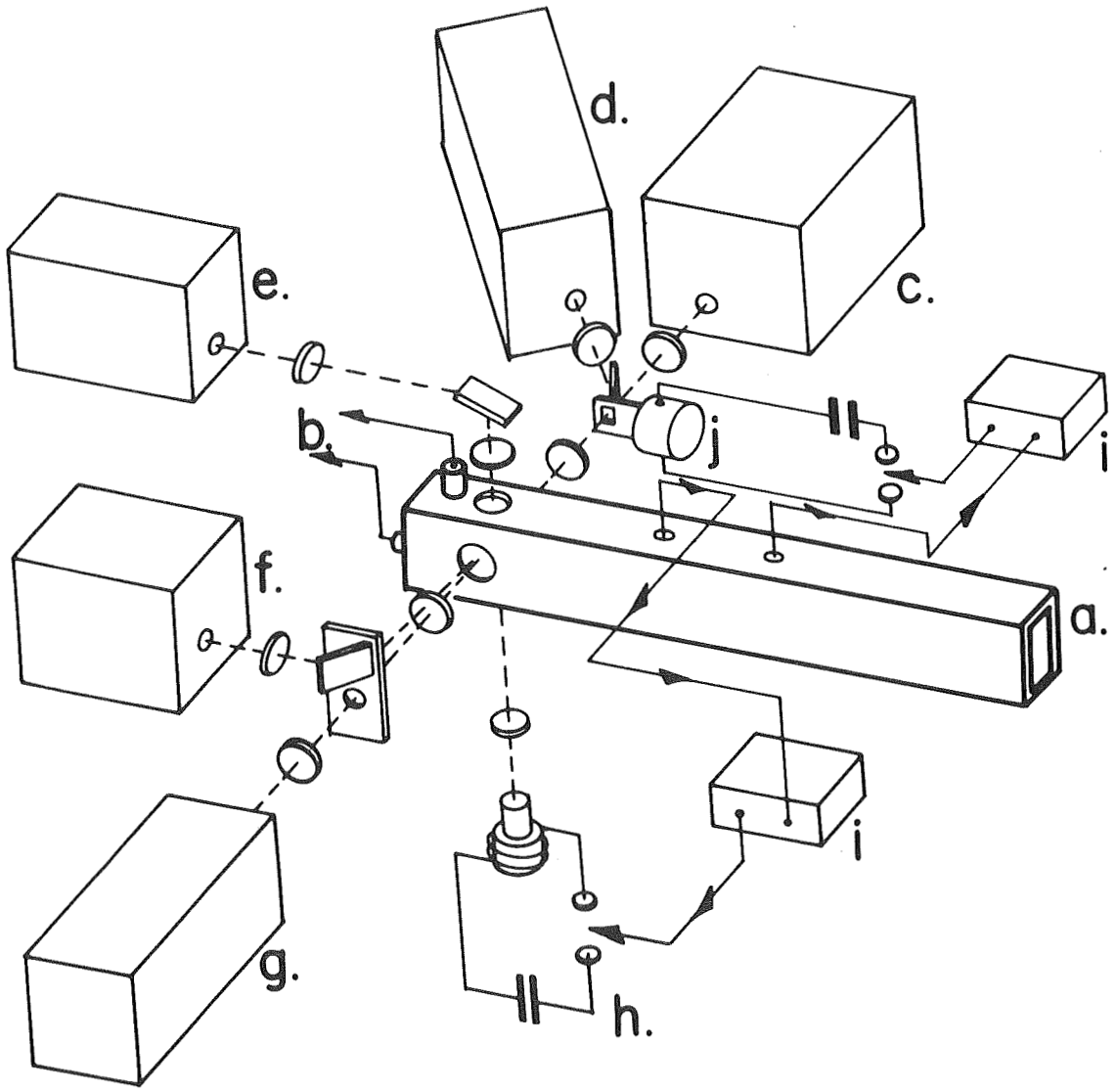

Figure 3. Schematic diagram of present instrumentation: a. shock tube test section, nominal internal dimensions 2.7" x 3.7"; b. quartz pressure transducers, one mounted in the end wall, and the second in the top wall, of the shock tube; c. 3/4 meter photographic spectrograph (f./6.3) with 2 Å resolution; d. 1 meter photographic spectrograph (f./8) with 0.25 Å resolution, e. 2-channel polychromator for reversal measurements; f. 12-channel polychromator for absolute intensity measurements; g. 4-channel polychromator for view ing selected lines (e.g. NeIλ5852) and their nearby continua; h. reversal flash lamp; i. time delay generators; j. fast shutter actuated by an exploding wire.

(ii) in later phases of the work, either spectrograph (c) or (d) could be employed with the fast shutter (j), but not both simultaneously, as is now possible.

Three polychromators (18 photoelectric channels) and two spectrographs (time resolved photographic recordings) view the hot gases in a single plane 2 cm upstream from the reflecting wall. The polychromator (e) viewing along a vertical axis monitors the wavelength band around 5,000 Å with 2 channels of 4 Å width, first in emission, and then in absorption against the continuum of the TRW flashlamp (h) which backlights the shock tube. Pairs of channels (spectrograph g) sample the spectrum at selected wavelengths to measure, for example, the integrated intensities (for shots where $T > 11{,}000°K$) of the neon line Neλ5852 and its background. A twelve channel image dissector composed of 50 μ thick microscope cover slides joined to fiber optic bundles samples 1 Å wide slices of the spectrum[32,45] (monochromator f). Spectrographs (d) and (c), have resolutions of 0.27 and 2.0 Å, and vignetting-free bandpasses of 1800 Å and 3000 Å, respectively. The mechanical shutter (j) is driven by an exploding wire and is located at an intermediate focal position.

Figure 4 shows a cut-away diagram of the shutter, which was developed for this work. Its use provides event-triggered emission and (absorption) "snapshots" over wide wavelength ranges. Simplicity and reliability are two important advantages of this design.[36] After a 60 μsec initial acceleration period, the moving slider attains speeds of 60 - 80 meters per second, depending on the size of the voltage pulse used to explode the wire: the slider is massive enough (1.1 g) to keep these speeds nearly constant for approximately 150 μs. Jitter in the delay before sampling (for a close-open-close mode of operation) is typically 6 - 8%. Because of the high velocity of the slider, the moving slits can be made wide enough to prevent stopping-down of high aperture optics occurs. Slits of 0.9 - 3.6 mm width were employed to give sampling times of 18 - 72 μs. Generally, the random variation in sampling times was 6-10%. Ralatively wide (3.6mm)

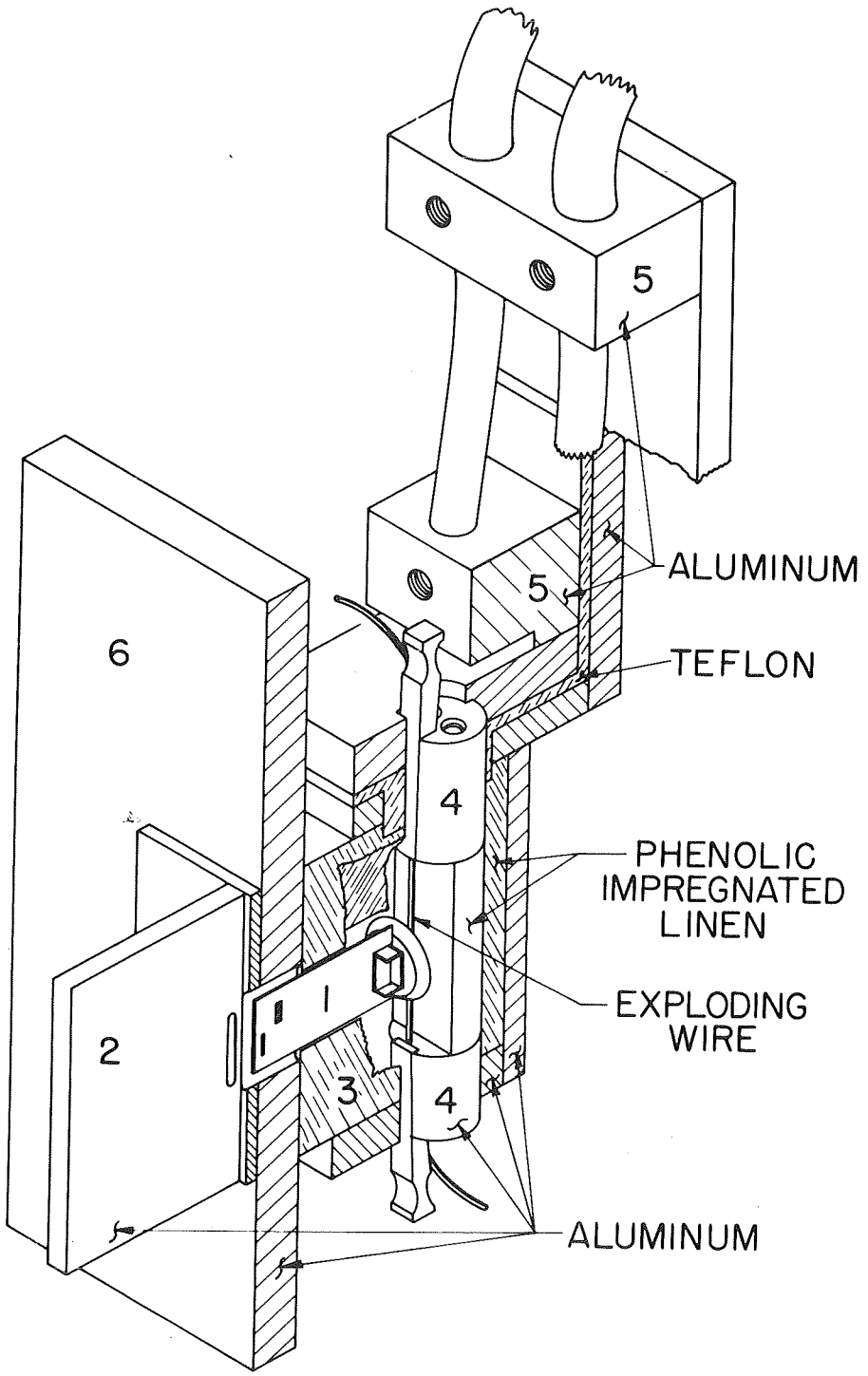

Figure 4. Cut-away view of the fast shutter preparatory to firing: 1. Slider bearing a pair of windows for sequentially framing the spectroscopic plasmas behind the first and multiply reflected shocks; 2. static slit assembly used for alignment of the shutter; 3. breech assembly through which the slider, 1., travels; 4. electrodes for securing the exploding wire; 5. high voltage connections; 6. mounting bracket and stop to arrest the moving slider.

slits provided optimal exposures for weak uranium shocks of long duration. Much shorter sampling times would be possible if the shutter were positioned very close to the spectrograph slit so that, say, 0.3 mm wide slits could be used on the slider.

The shutter is now positioned at a common intermediate focus of two spectrographs, so it can serve both simultaneously. The high resolution instrument (d) is reasonably stigmatic, so that a framing mode is obtained by employing a pair of slider slits which are off-set both vertically and horizontally. Photomultipliers within spectrographs (c) and (d) were used to correlate photographic sampling times with data from polychormators and pressure transducers. Quartz pressure transducers are flush-mounted in the side and end walls. A series of spark gaps is used to measure the incident shock speed and to start delay generators for triggering the flashlamp, the fast shutter and the various CRO sweeps.

Absolute calibration of photomultipliers at $\lambda = 6563$ Å was performed both in the conventional way, using the anode crater of a well-regulated DC carbon arc,[23] and by a new method which utilizes the A-value and Stark profile of H_α as fundamental standards.[26] These two sets of calibrations agreed to 5% , which was felt to be the tolerance of either method separately. Photomultipliers at other wavelengths were calibrated with the carbon arc. Optically thick, "gray body" radiation from shocks in argon-xenon mixtures was employed for checking that all photoelectric channels on the various spectrographs were registered on the same absolute sensitivity scale. Films (Kodak 2475, 103-0, HSIR) were calibrated for spectral response with the carbon arc, and their characteristic curves (density vs $\log_{10}$ exposure) were determined with the carbon arc. Various bright, transient light soruces were also used for this purpose, as a precaution against reciprocity failure. Absolute sensitivities were determined for each experimental run by fitting the signals from 8 - 12 calibrated photomultipliers (spectrograph e) to the corresponding photoelectric signals.[32,33]

B. Test Gas prepartation

Methods for preparing and handling the test gases appear, in retrospect, to have left compositional nonuniformities in the mixtures of UF_6 and neon. Several refinements have been made, and more improvements are underway.

Initially, 2 - 20 torr of UF_6 were admitted to a 0.2 liter Monel tank, to which was added 1000 torr of Research Grade neon. After several minutes, the mixture was drawn into the evacuated shock tube, which was fired 1 - 2 minutes thereafter. The inadequacy of this technique was soon apparent because, at essentially constant incident shock speed, the spectroscopic variables were not reproducible functions of the supposed initial UF_6 concentrations. Analysis of the data showed a factor of 2.2 scatter in measured absolute mass absorption coefficient. Preliminary checks had given no indication that 20 torr of UF_6 would either decompose or be absorbed in periods ranging up to several hours.(37) Therefore, it appeared that incomplete mixing of the test gas constituents might be at fault.

Working on this assumption, the mixing and metering apparatus was modified to eliminate the most obvious sources of possible test gas inhomogeniety. Valves were installed so that the two Wallace and Tiernan absolute pressure gauges could be isolated from the mixing chamber. The inlets to these gauges are fitted with small constrictions as surge protection. Since the combined volume of the two gauges was comparable to that of the mixing chamber itself, it appeared plausible that, depending on how the neon flowed into the flask containing uranium hexaflouride, there could be different UF_6 concentrations in the gauges and the mixing chamber proper. In addition, large polished steel balls, which could roll freely in the chamber, were used to stir the mixtures. These modest precautions effected a three-fold reduction in scatter for the measured absolute mass absorption coefficients.

Scatter for the data reported here is 40 - 50% (equivalent to a factor of 2 between extremes). It is felt that further refinements in mixing procedures are feasible and these are expected to further reduce the scatter.

C. Plasma Pressure

Pressures measured by the side wall transducer agreed within estimated tolerances with those from the end wall transducer. These data are shown in Figure 5. The 8% scatter (σ) between the two measurements can be attributed to ringing in the piezoelectric crystals and to the reading error. One gauge read systematically 8% higher than the other. The same gauge continued to read high when positions of the gauges in the tube were interchanged. This slight inconsistency persisted when the gauges were recalibrated. The average of the two measured pressures should be good to ±6% in a typical experiment.

D. Temperature Measurement

Two independent determinations of temperature were made using the "reversal" technique. The same two photomultipliers used to determine the plasma emissivity at 5,000 Å and 5,200 Å via equation (3), were used for thermometric purposes. Each of the absolute calibrated photomultipliers has a bandpass of 4 Å and records the reversal (black body) intensity at its own wavelength. The Planck function

$$B(\lambda,T) = 2h\nu^3/c^2 \; 1/e^{h\nu/kT-1}$$

is then solved for temperature. So long as the shock tube plasma is homogeneous, the validity of this equation requires only that the flashlamp radiation be locally gray over the 4 Å bandpass. From equation (2) it can be deduced that the structure of the shock tube spectrum emission does not effect the validity of the method. In practice, the mean value of $[1 - e^{-\tau}]$ should be greater than 0.3 for good precision in observing the reversal on a standard CRO. Temperatures measured by the two photomultipliers, one at 5000 Å and the other at 5020 Å, are compared in Figure 6. For the majority of experiments, the two determinations

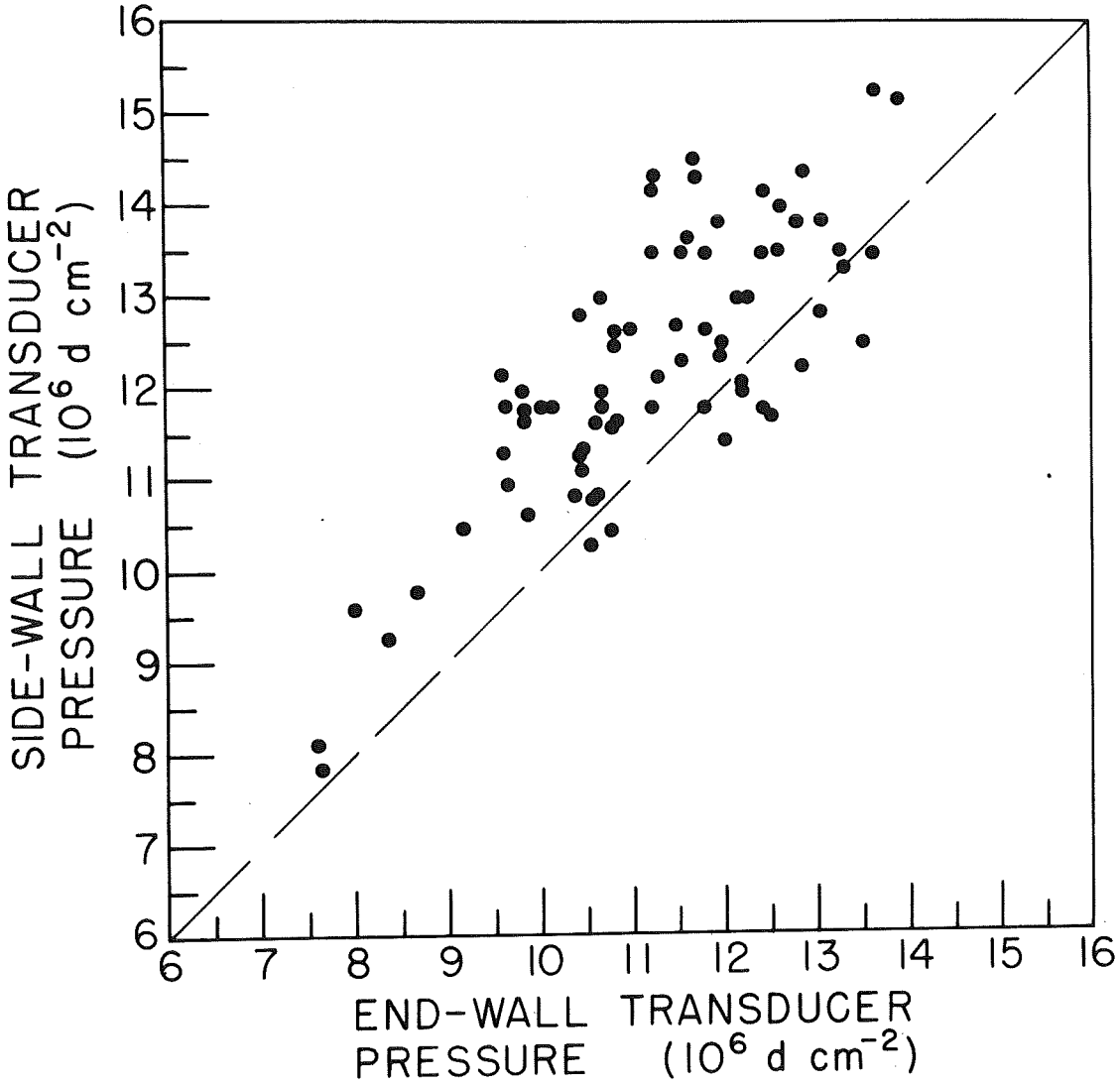

Figure 5. Comparison of plasma pressures obtained from the side-wall and end-wall transducers.

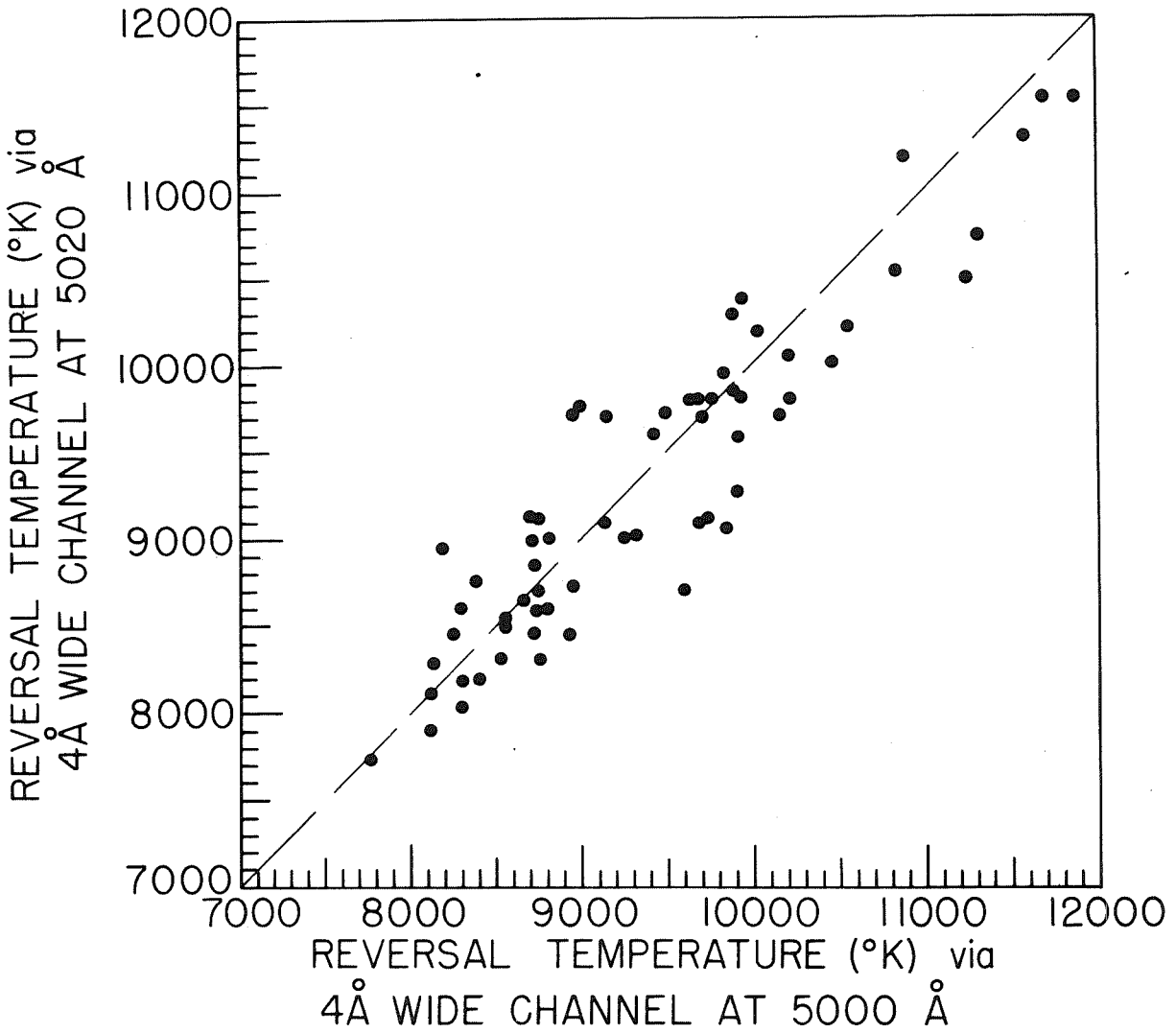

Figure 6. Comparison of reversal temperatures measured simultaneously at 5000 and 5020 Å .

agreed within 5% . An a priori estimate of the precision for either measurement separately is 4% .*

Temperatures derived from the theory of shock tube operation (Rankine-Hugoniot relations) and the measured incident shock speed[10-13] proved to be of qualitative value only. By applying the conservation laws for mass, momentum and energy to the jump-conditions across the shock front, it is possible to predict the thermodynamic conditions behind shocks of known speed - subject, of course, to the validity of a one-dimensional model for the shock tube. Such predictions have been tested on several occasions.[34,38,39] It has generally been found that the predicted temperature was particularly sensitive to non-ideal shock tube behavior such as boundary layer growth, weak diagonal shocks, and

---

*In the strongest, lowest uranium content shocks, the neon line Neλ5852 attained sufficient brightness to allow good recording and to make insignificant possible contributions from overlapping uranium lines. Using the absolute integrated line intensity I, (recorded photoelectrically and, in a few instances, photographically as well) and measured pressure, we obtain a temperature

$$N(p,T) = I \cdot 4\pi\lambda / hc\ell A$$

where $N(p,T)$ is the number density of neon atoms in the relevant excited state, A is the transition probability and ℓ is the thickness of the emitting gas. Because of the statistics of Boltzmann equilibrium $N(p,T) \sim e^{-E/kt}$, where E is the excitation energy of the line. Calculated Stark broadening parameters are used to make small corrections for optical depth and the effects of both finite slit width and the proximity of the line and near-continuum channels.[44] However, these corrections are of marginal significance, as is the 10-20% uncertainty in the A-value of NeI5852 because, with $E/kT \sim 20$, the line brightness is very sensitive and primarily so to temperature. Reduction of these neon excitation temperatures, which will be available for approximately 5 - 10% of the experiments, is still in progress. When completed, this temperature will be compared with reversal temperatures as a test for self-consistency. Because relatively few neon temperatures will be available, and because numerous prior studies[32-34] have shown neon and reversal temperatures to be of equivalent accuracy, no significant changes are anticipated in the mass absorption coefficients already reduced.

poor initial shock formation. Typically, predictions based on shock speed tend to fall 1 - 6% lower than directly measured temperatures, depending upon the performance of a particular shock tube and the type of test gas used.

The comparison made in Figure 7 between the measured (2 reversal) temperatures and temperatures predicted from shock speeds indicated that the latter are not reliable enough for quantitative spectroscopic use, but may be helpful for understanding the radiative gas-dynamic aspects of these optically thick plasmas. The tendancy for the predictions to underestimate temperatures is due in part to the influence of boundary layers. However, the same apparatus was used in studies of light elements (eg. CH_4, CH_3Br, SiH_4), over a similar range of spectroscopic additive concentrations, and these (optically thin) plasmas do not depart so drastically from predictions as does uranium. Radiative cooling is probably responsible for much of the failure of the predictions for the optically thick uranium plasmas. It will be seen later that the emissivity of uranium plasmas increases approximately as the concentration to the 3/2 power. Therefore, if the temperature remains constant, a 2% UF_6 mix should cool 8 times faster than a 1/2% mix. However, due to greater amounts of energy required for dissociation, the rich mixture is typically 2,500°K cooler than the lean one. Therefore, we expect the 2% mix to cool about $8 \times (10{,}500/8{,}000)^{-4} \approx 2.7$ faster than the lean one. Figure 7 indeed shows that the temperature discrepancy increases from 15% to 32% in going from .5% to 2.0% concentrations of UF_6. The loss rates cannot be calculated analytically without detailed knowledge of wall reflectivity versus wavelength and good estimates of the emissivity below 2800 Å. Additional evidence for progressive cooling of shocks in a 1.6% UF_6 mixture is given in discussion of Figure 11.

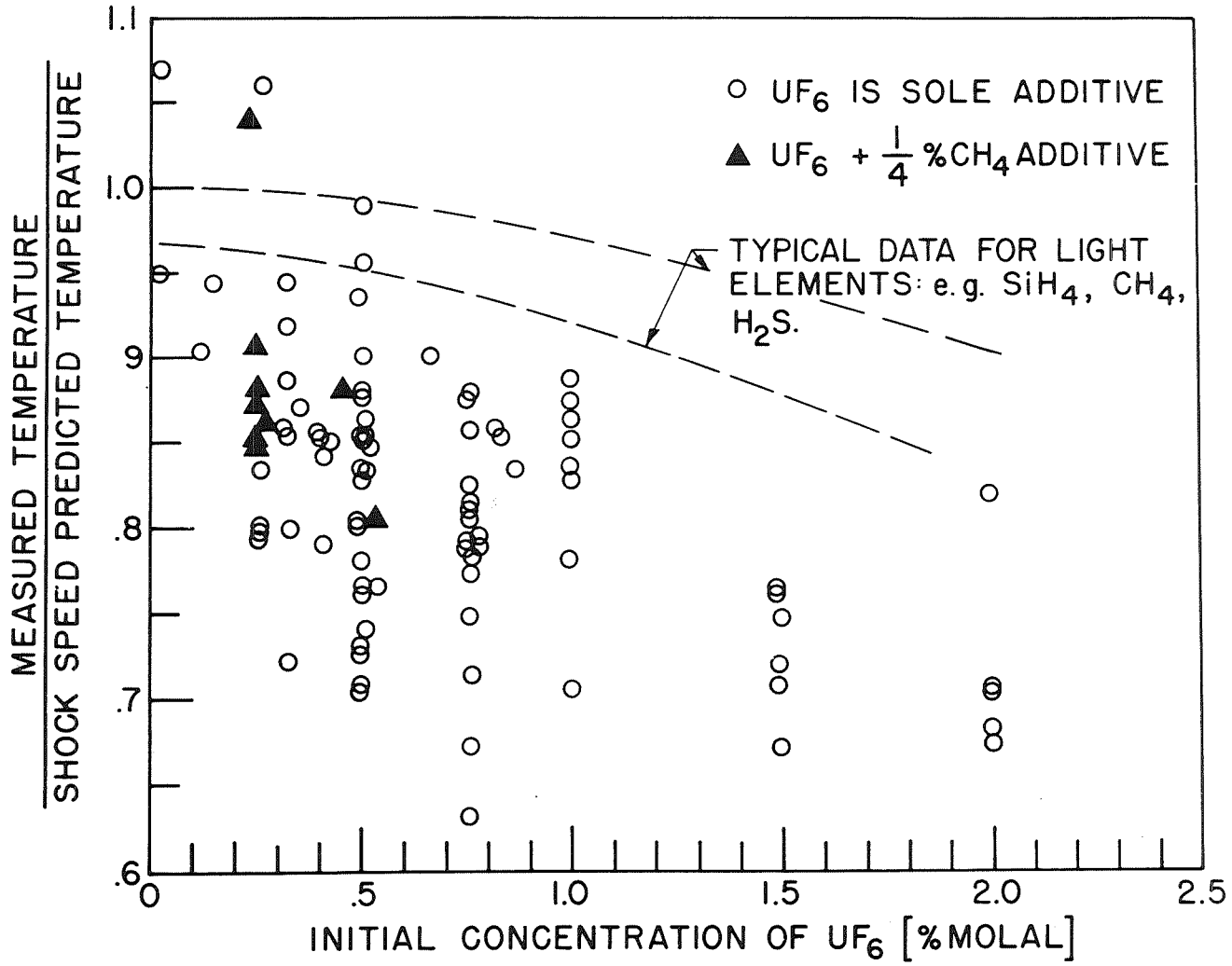

Figure 7. Ratio, measured temperature/temperature predicted from measured incident shock speed, as a function of the test gas UF_6 concentration. The predictions ignore radiative cooling. The trend for the predicted temperatures to be grossly too small for rich UF_6 concentrations is consistent with the finding (Section IV) that the plasma emissivity has a stronger than linear dependence on the density of uranium atoms.

E. Electron Density

Electron density was measured for a relatively few experiments which offered the best chance of observing Stark broadening of UI lines. For these runs, 1/4% CH_4 was added to 0.2 - 0.3% UF_6 in neon. Low UF_6 concentrations were used for the following reasons:

(i) to avoid complications from high optical depth,

(ii) to keep the continuum low enough so that profiles of H_β could be measured with reasonable accuracy,

(iii) to maintain the temperature required to give good overall brightness to H_β .

The electron density is obtained by fitting the observed H_β profiles, to the theoretical[40] Stark profiles. Previous experience[29,41,32] has shown that the precision of the method is typically 15% , and that electron densities deduced in this way are not readily prone to serious systematic bias.

F. Intensity and Emissivity Measurements

Before considering the emissivity data obtained by the emission and absorption techniques, it should be stressed that the observed radiation is due almost entirely to uranium (UI , UII , UIII) and free electrons. Prior studies with this apparatus have shown that the lines of flourine are not excited to detectable brightness when temperatures are less than 12,000°K.[33] The emission spectrum of neon becomes discernable above 10,500°K , but it is limited to a few narrow, well-known[43,44] lines in the red and near infrared.

It also bears mentioning that the resonance lines of neutral uranium cannot readily be studied with the shock tube because of the problem of re-absorption in cooler boundary layers. Depending on how far boundary layer growth has progressed before photographic exposures are made, these lines can be

seen either in emission or in absorption against the continuum. From the standpoint of the present emissivity studies, it is therefore fortunate that the UI resonance lines constitute only a very small fraction of the identifiable lines in the wavelength region 3000 - 9000 Å.

Emission data from a single shot for the region 4960 - 5000 Å are shown in Figure 8. The scatter between the 6-9 photomultipliers, each viewing a different 1Å wide portion of the spectrum, indicates the "gapiness" of the spectrum seen with this bandpass. The relative scatter decreases with increasing absolute intensity because slit-averaged emissivities approach a common limit of unity. The emissivity for each run shown in Figure 9 is determined by dividing the slit-averaged intensity, $B_{avg}(T)[1 - e^{-\tau}]_{avg}$ by B(T), the Planck function computed from the measured temperatures. In Figure 9, the data from one photomultiplier (#3) are systematically larger than from the others. Data from this channel are suspect because as emissivities approach unity, this channel measures black body intensities that are significantly higher than those obtained by all other channels.

Slit-averaged emissivities at 5000 and 5020 Å, obtained by the pair of 4 Å wide reversal intensity channels, are compared in Figure 9. Inasnuch as the reversal temperatures measured by these channels have been shown to agree well, any differences in the plasma brightness at the two wavelengths can be ascribed to differences in local values of $[1 - e^{-\tau}]$. The two sets of emissivities in Figure 10 fit rather convincingly to the agreement obtained if slit-average optical depths at 5000 Å are 1.3 greater than at 5020 Å.

Figure 10 compares emissivity, $I/B(T) = [1 - e^{-\tau}]_{avg}$, obtained emission measurements against the (average) emissivity measured by the two

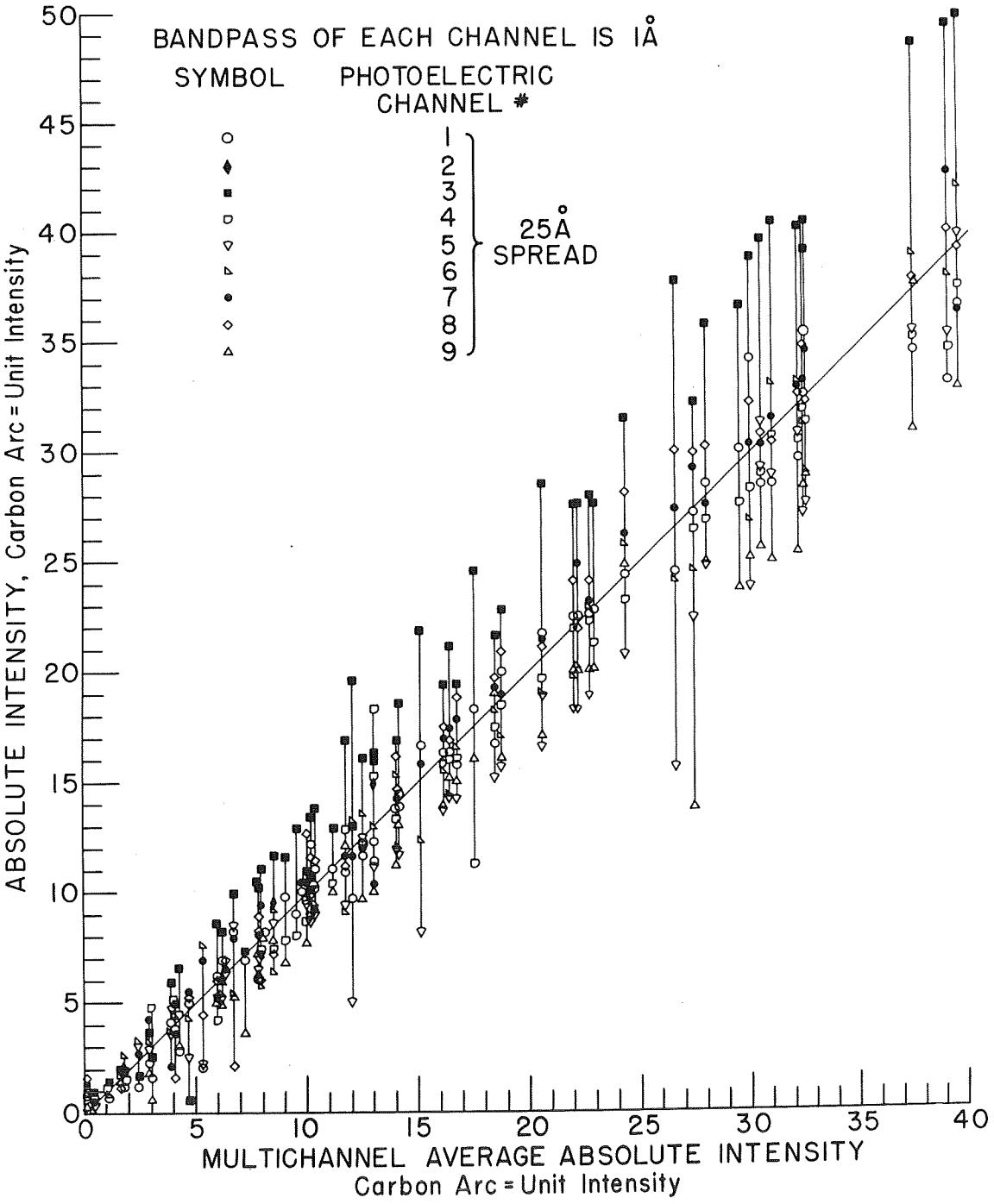

Figure 8. Comparison of absolute intensities (in units of local carbon arc intensity) measured by 9 independent photoelectric channels with the average of the measured intensities.

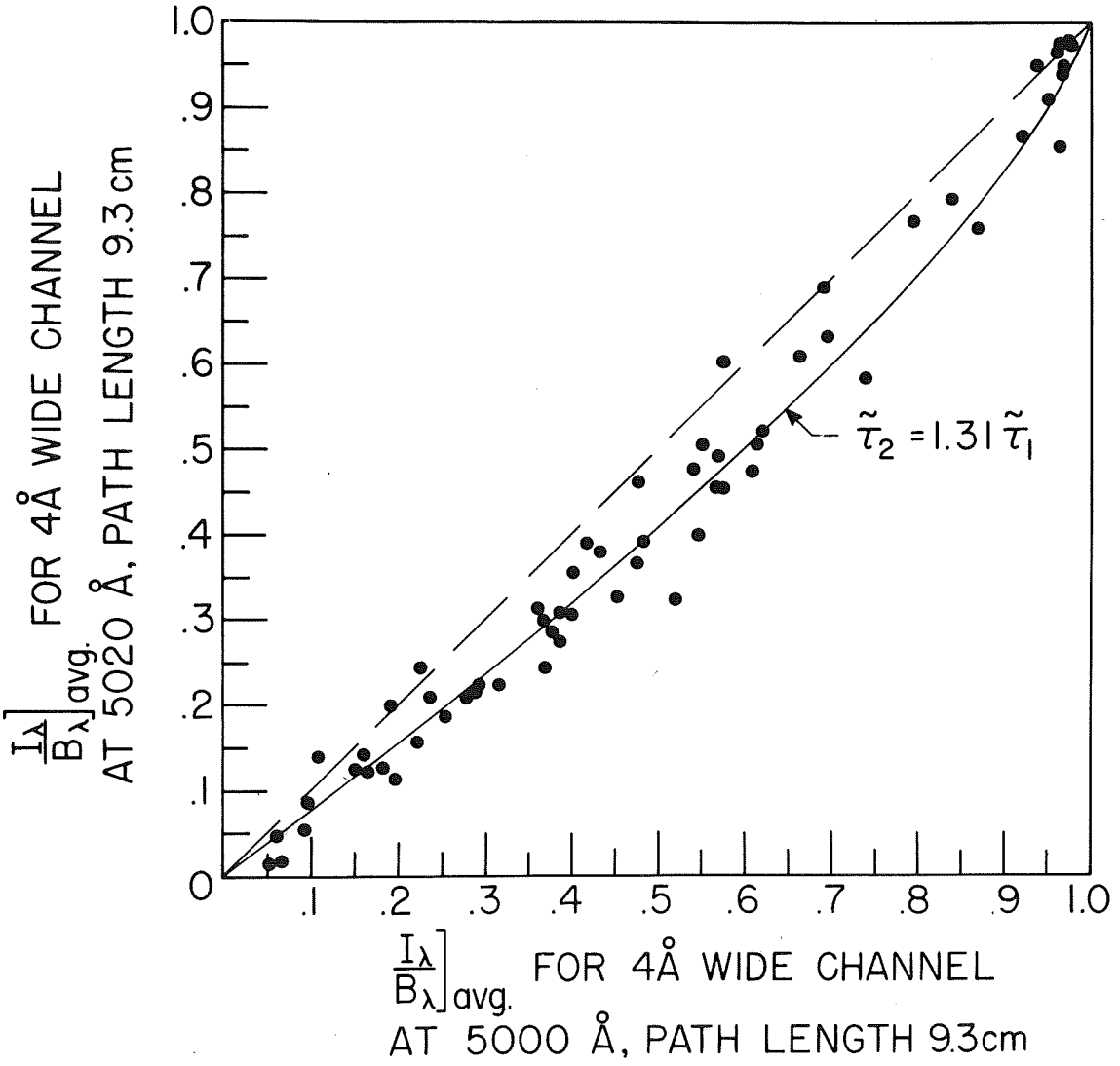

Figure 9. Comparison of slit-averaged emissivities $\frac{I\lambda}{B\lambda}$ avg. , from simultaneous reversal measurements at 5000 Å and 5020 Å .

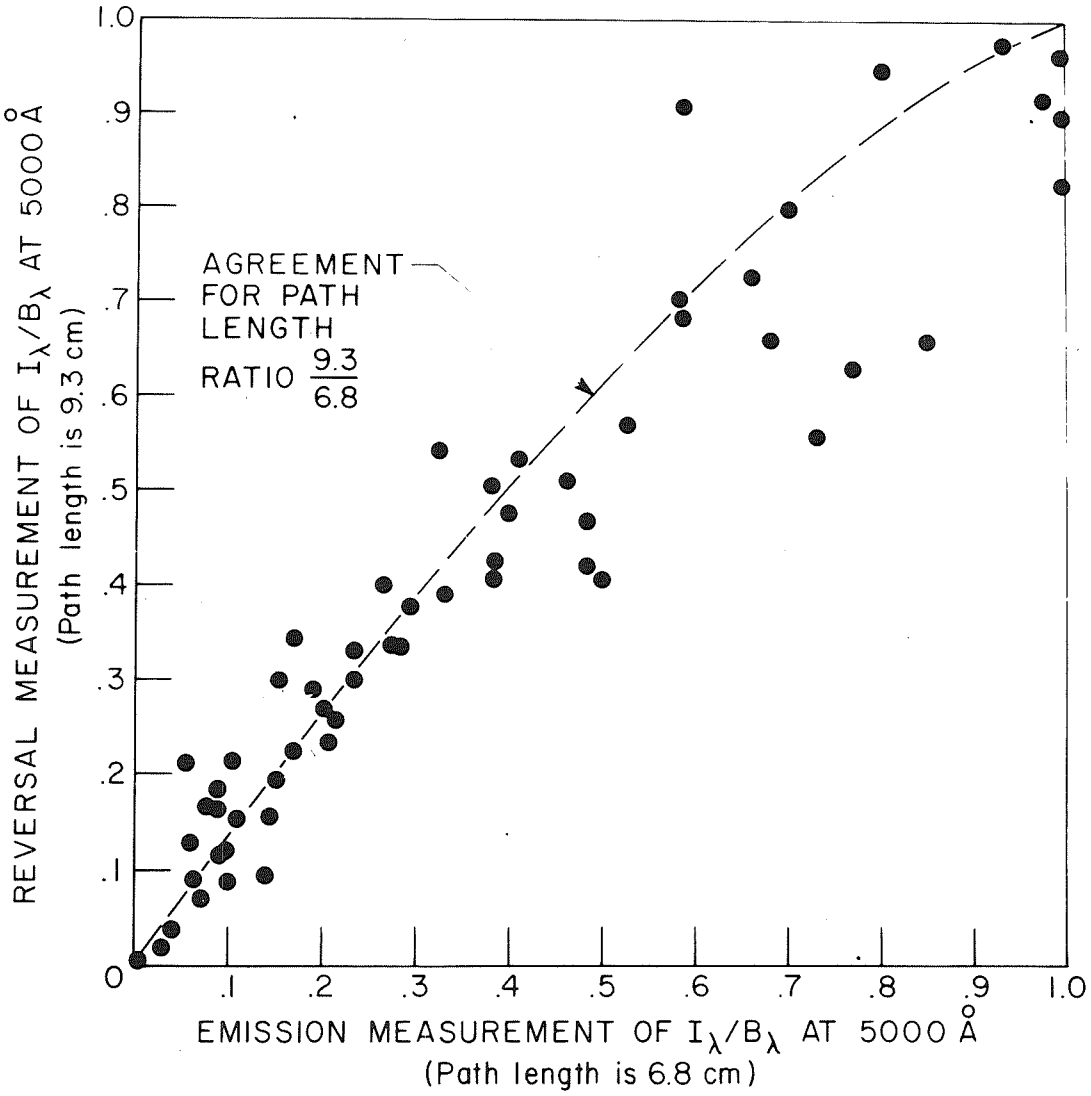

Figure 10. Comparison of emissivities, $I\lambda/B\lambda$, at 5000 Å measured in absolute emission and by the line reversal technique.

reversal channels. Agreement is excellent over most of the range, once one takes into account the different path lengths viewed by the reversal and the emission channels.

The structure of the uranium spectrum, and the variation of emissivity with wavelength, was investigated using photographic recording. Initially, we used 70 mm wide rotating-drum films, such as the one shown in Figure 11. In later phases of the experiments, regular 4" x 10" spectroscopic plates (as in Figure 12) were employed with the aid of the fast shutter. If the plasmas were everywhere optically thin, then the variation of the absorption coefficient with wavelength would be proportional to the distribution of spectral intensities. If absolute intensities I and the temperature T are known, one can reconstruct a spectrum to its appearance in the optically thin limit, provided that the instrumental width is small compared to the widths of all spectral features. This is accomplished by treating the apparent intensity at all wavelengths to the correction

$$\tau/[1 - e^{-\tau}] = - \frac{B(T)}{I} \ln[1 - I/B(T)] \quad . \qquad (5)$$

Although the condition of good resolution is not satisfied in the present experiment, we still use equation (5). This provides opacities for the continuous and semi-continuous portions of the spectrum and at least partially compensates for self absorption in the lines. The three drum-camera spectrograms shown in Figure 11 cover the same wavelength region, 5000-6050 Å, but corresponds to different UF_6 concentrations. Dispersion and resolution are 20 Å/mm and 1.2 Å , respectively. Writing speed is approximately 0.09 mm/μs . Evidence for progressive cooling by radiation can be seen in spectrogram C. The four spectrograms shown in Figure 12 were obtained with the fast shutter for shocks

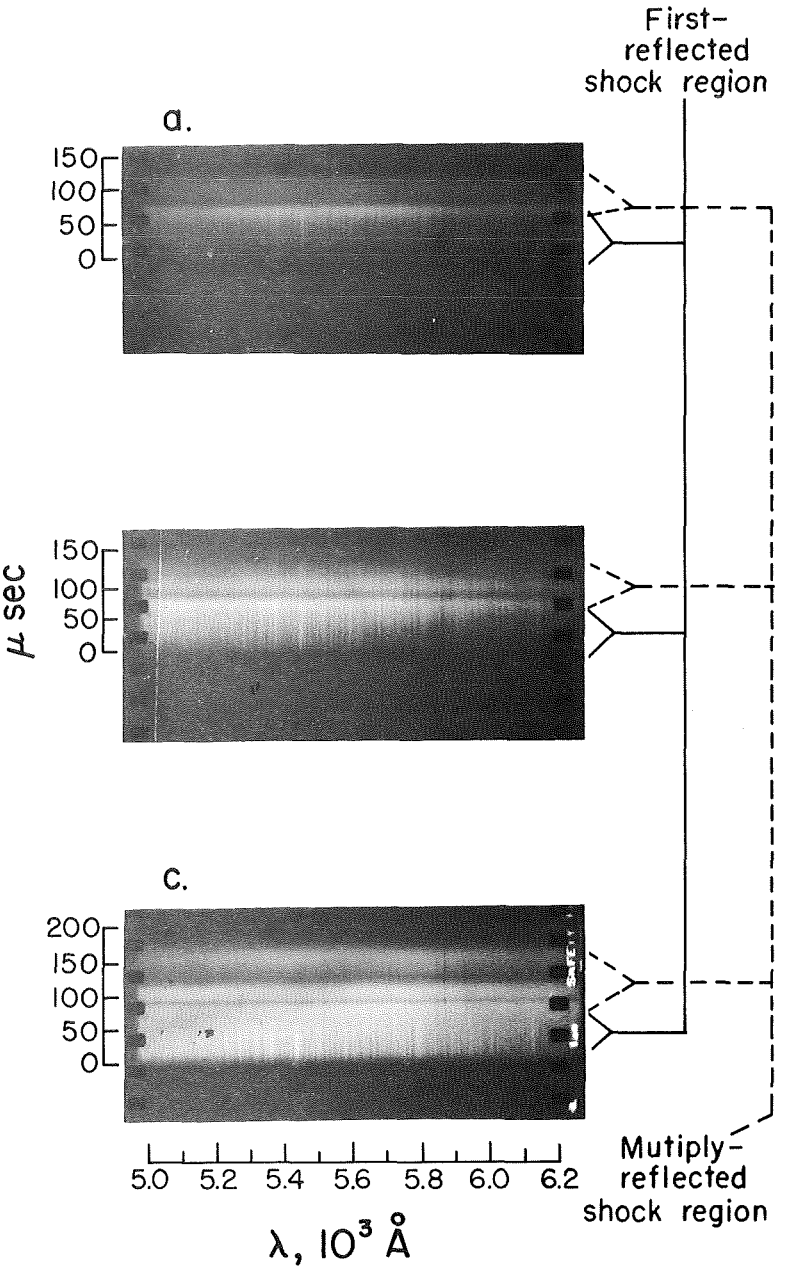

Figure 11. Sample uranium spectra obtained with the rotating-drum camera. The vignetting-free wavelength coverage of the 70 mm film (Kodak 2475) is 1050 Å. The origins of the time axes are the instants when the reflected shock wave passes into the spectroscopic line of sight. These three spectrograms show the effect of progressively increasing the uranium concentration: for a., b., and c., uranium partial pressures are 2.8 , 4.9 and 8.6 X 10^4 d cm^{-1} , respectively. Late in the first reflected shock region of c., the spectrum becomes featureless. This is attributed to radiative cooling. By 1) increasing the mass absorption, 2) increasing the density of uranium (at constant pressure), and lowering the local Planck intensity, this causes emissivities to tend towards unity.

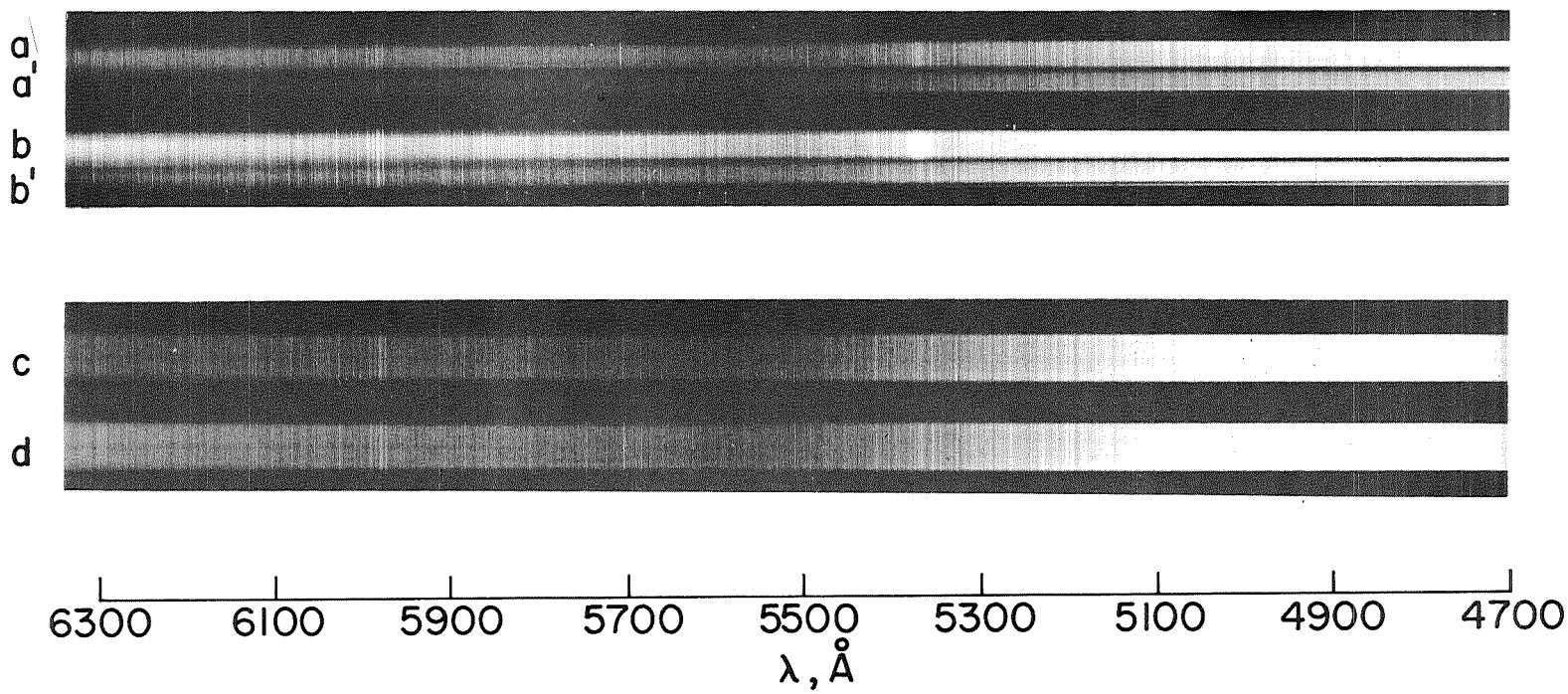

Figure 12. Sample uranium spectra obtained with the fast shutter. Exposure times are 40-46 μ sec. For spectrograms a., a'., and b., b'., the shutter was employed in a framing mode to sequentially sample two plasma regions in a single shock tube experiment. For c. and d., only a single exposure was made per experiment. Initial UF_6 concentrations were 1.1% for a., a'.; 1.4% for b., b'.; 0.38% for c. and 0.46% for d.

in various mixtures of UF_6 in neon. Exposure times were 40-46 μs. Resolution is slightly better than 0.3 Å at the low wavelength end of the spectrograms.

The CRO data from a single shock tube run, along with pertinent annotations are given in Figure 13.

IV. Results and Discussion

a. Absolute Emissivity (and Opacity)

The data in Figure 14 are slit integrated emissivities,

$$I/B(T) = (\Delta\lambda)^{-1} \int_{-\Delta\lambda/2}^{\Delta\lambda/2} [1 - e^{-\tau}] d\lambda$$

obtained by averaging the emission and reversal determinations for the range 4,960 - 5000 Å. In lieu of a three dimensional plot showing these data as functions of both number of uranium atoms and temperature, Figure 15 collects results from within 1000°K intervals and denotes them by different plotting symbols. In spite of the bothersome scatter, it can be seen that the data from the various temperature ranges behave in distinctive ways. (The thermal dependence of emissivity is seen more clearly in representations such as Figure 16.)

Scatter (σ) in the data for a given temperature range is typically 40%. Several previous experiments involving absolute photometry of light elements has conditioned us to expect less than 1/2 this much scatter. Random error of ± 4% in temperature is expected to generate 10 - 12% fluctuations in the Planck function B(T). However, this is of secondary importance in comparison with the scatter from some unspecified source. We believe the random generator to be test gases inhomogeniety. A skeptical interpretation would be that one can only err systematically downward, i.e., get less UF_6 than one supposes. As indicated previously,

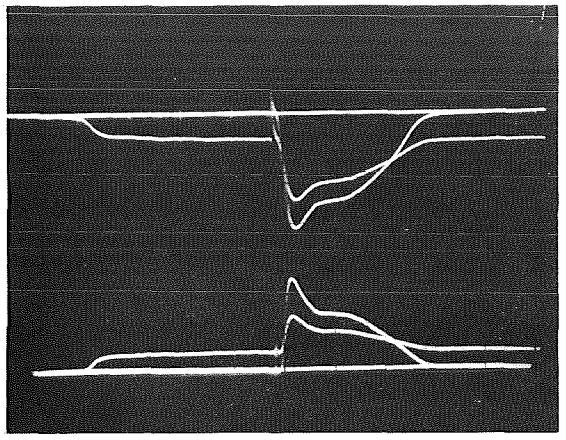

UPPER BEAM: Reversal channel at 5000 Å. The intensity trace from the shock tube plus the flashlamp is superimposed upon a trace of the flashlamp alone (20 μ sec cm^{-1}).

LOWER BEAM: Reversal channel at 5020 Å. Inverted intensity trace of the shock tube plus the flashlamp is superimposed upon a trace of the flashlamp alone (20 μ sec cm^{-1}).

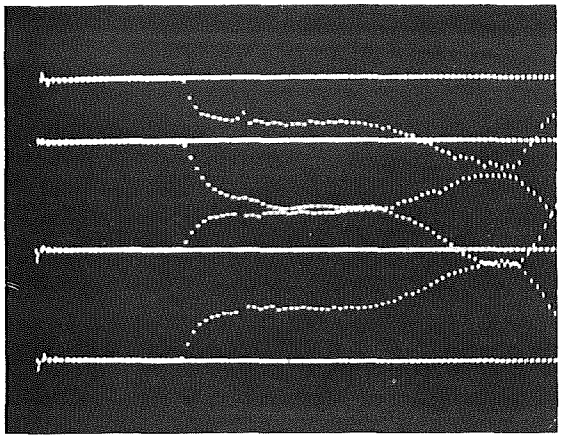

Signals from four photoelectric channels, centered at (top-to-bottom): 4960 Å, 4961 Å, 4962 Å, 4964 Å. Bandpass of each channel is 1.0 Å. The two lowest traces are inverted. Common sweep speed is 50 μ sec cm^{-1}.

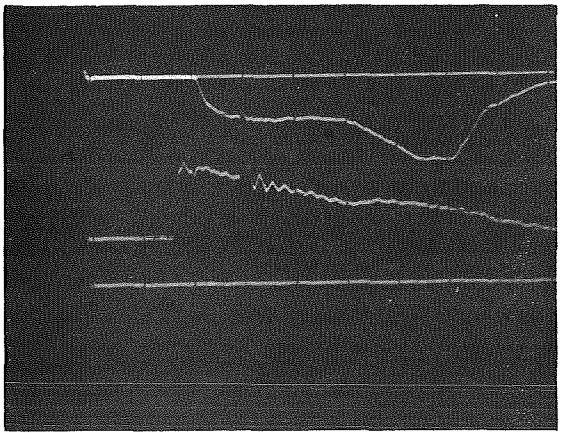

UPPER BEAM: Photoelectric channel (1.0 Å bandpass) centered at 4959 Å.

LOWER BEAM: Output from pressure transducer mounted in shock tube's end wall. Apparent decrease of pressure with time is instrumental - plasma electron densities cause charge leakage from the piezoelectric crystal. Sweep speed for both beams is 50 μs cm^{-1}.

Figure 13. CRO data from a single shock tube experiment. Measured plasma conditions behind first reflected shock are; T = 8300 ± 300 °K, uranium partial pressure = 7.6 X 10^{4} d cm^{-2}.

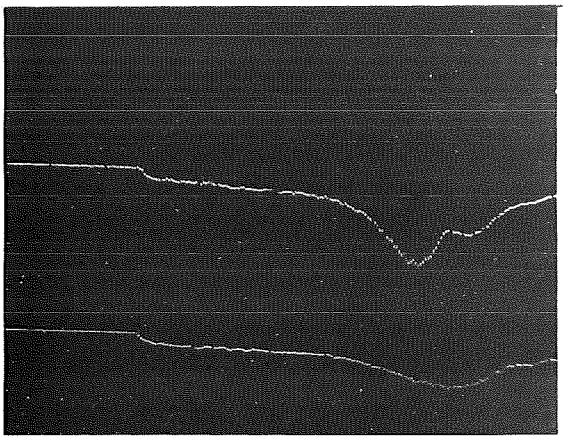

UPPER BEAM: Intensity from a 2 Å wide photoelectric channel, centered on 5852 Å to record the integrated intensity of NeIλ5852 (together with the continuum at that wavelength.)

LOWER BEAM: Intensity from a 2 Å wide photoelectric channel, centered on 5846 Å to record the local continuum of the line NeIλ5852. Sweep speed for both beams is 50 μ sec cm^{-1}.

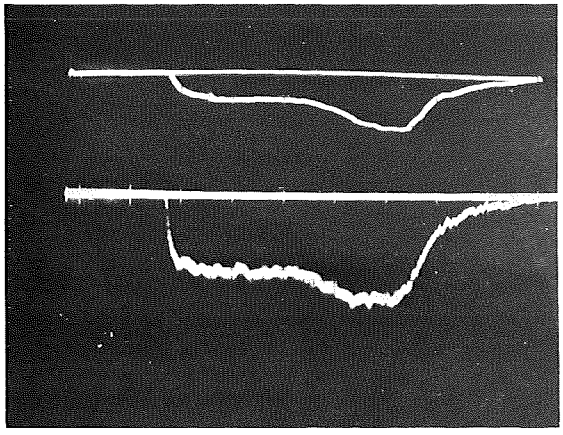

UPPER BEAM: Intensity from a 1 Å wide photoelectric channel centered on 4968 Å .

LOWER BEAM: Intensity from 4 Å wide photoelectric channel centered at 4200 Å. For thedepicted experiment this data is not of quantitative value because the photomultiplier has begun to saturate.

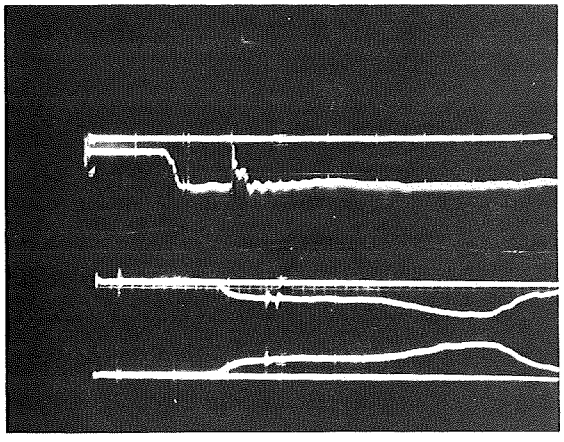

UPPER BEAM: Output from the pressure transducer mounted in the top wall of the shock tube.

LOWER BEAMS: Intensity from two 1.0 Å wide photoelectric channels, centered at 4955 Å , and (inverted trace) at 4957 Å .

Figure 13. (continued)

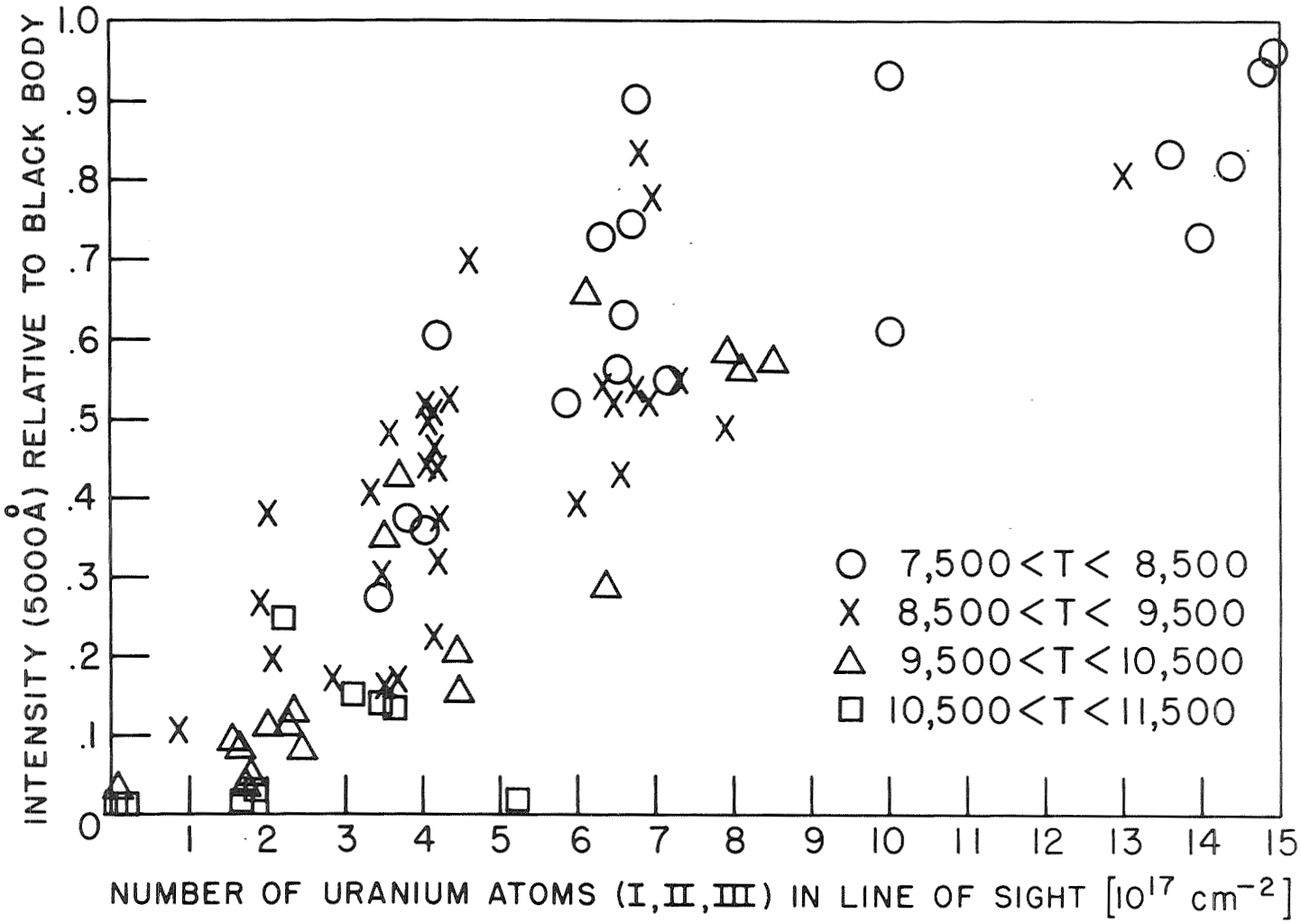

Figure 14. Uranium emissivity at 5000 Å as a function of the number of uranium atoms in the line of sight. Plasma temperature is shown as a parameter by grouping the data into four 1000° K intervals. Emissivities (intensities relative to a black body) represent an averaging of results from reversal measurements (two channels of 4 Å bandpass) with those from absolute intensity measurements (6-9 channels of 1 Å bandpass).

however, we believe that inadequate preparation can lead to gases which may be locally richer or poorer in UF_6 than one would calculate using measured initial partial pressures. Bremsstrahlung contributions - being due to the mutual action of electrons and ions - will scatter by 20% if the uranium concentration reproduces to 10% . Taking account of the tolerance in B(T) and the spread in data due to lumping into 1000°K intervals, we estimate that random fluctuations of 15% in UF_6 concentrations could fully account for the scatter shown in Figure 15. Photometry would not appear to contribute substantially to the scatter since the two independent techniques for measuring absolute emissivity were seen to give satisfactorily self-consistent results. Because UF_6 contains no hydrogen, the spectroscopic techniques we have used the past to test assumptions concerning the composition and thermodynamic state of the plasmas[32,35] could not be applied to the uranium data.

The "mean optical depths" shown in Figure 15 were derived from the measured emissivities (Figure 14) by applying equation (6). Small corrections (5 - 10%) have been given to these data to partially correct for the self absorption of strong lines (Section IIC). A logarithmic representation of τ_{avg} versus number of uranium atoms, N_U , is shown in Figure 16. If the opacity were due exclusively to discrete transitions, then τ_{avg} would have a linear, or weaker,[46,47] dependence upon N_U . If, on the other hand, Bremsstrahlung and recombination emission are the dominant contributors, τ_{avg} should scale as N_U^2 .[19,20] Data from within all four temperature regimes are seen to fall between the curves (slopes of 1.0 and 2.0, respectively) for these idealized cases. That is, contrary to theoretical predictions, line and continuum radiation appear to account for comparable fractions of the total opacity. In the next section it will be seen that photographic data also indicates that continuum and

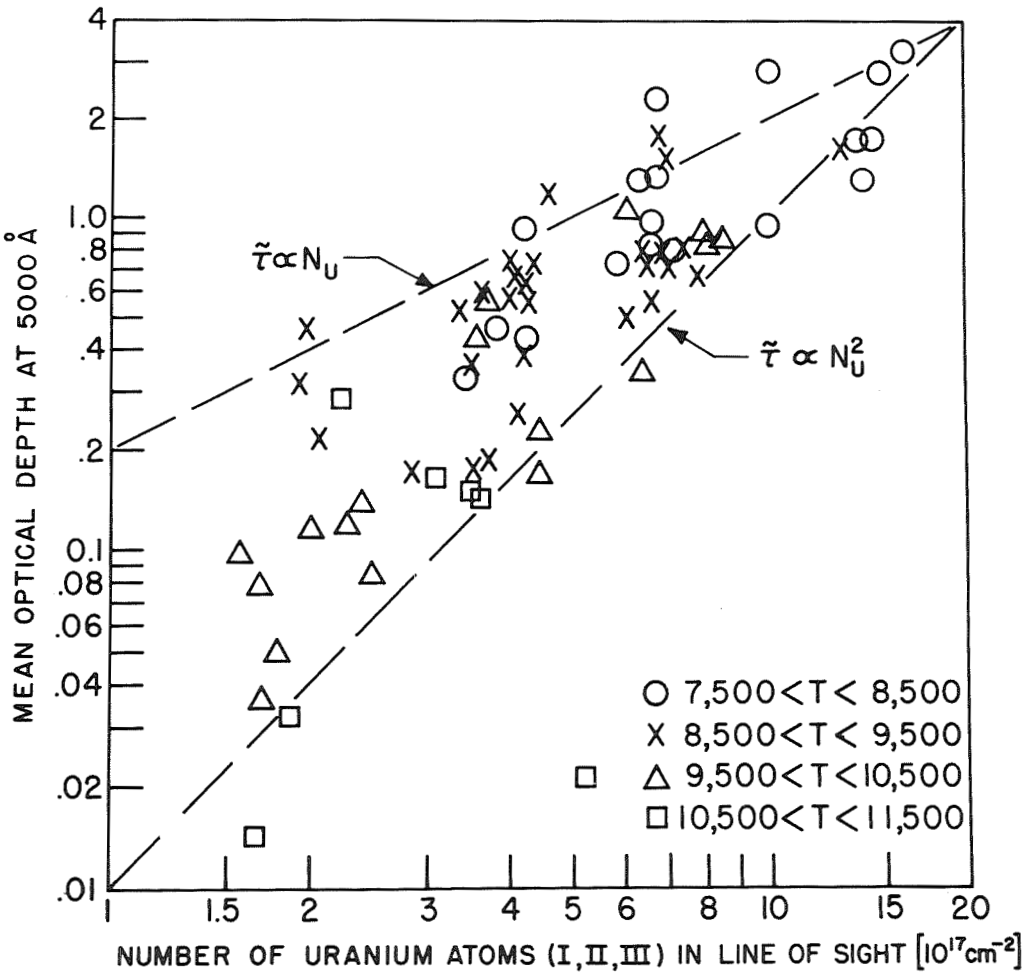

Figure 15. Mean optical depth $\tilde{\tau}$ of uranium at 5000 Å as a function of the number of uranium atoms in the line of sight. Temperature is shown as a parameter by grouping the data into 1000° K intervals. Curves indicate the behavior expected if the plasma radiation were optically thin and due exclusively to either lines ($\tilde{\tau} \propto N_U$) or continua ($\tilde{\tau} \propto N_U^2$).

line radiation are of similar importance. Data for $\tau_{avg} > 2$ are relatively reliable because small errors in the measured variable $(1 - e^{-\tau})$ lead to large errors in τ_{avg} as $(1 - e^{-\tau})$ approaches 1.0. The theoretically predicted trend for τ_{avg} to decrease with increasing temperature (at fixed N_U) is clearly discernable.

Absolute results to date are summarized and compared to theory in Figure 16. Predicted contours of equal opacity (at 5000 Å) are plotted as functions of temperature and uranium partial pressure. The hatched-in areas represent the current data and incorporate ± 45% tolerance limits. The depicted data span most of the p-T domain that is consistent with both reasonable spectroscopic signal levels and normal gas driven shock tube operation. Agreement with theory improves with increasing uranium partial pressure, and to a lesser extent, with increasing temperature. Because the theory is partially statistical in nature, it is expected to do better under these conditions (higher T and uranium partial pressure) that excite the lines of UI, UII and UIII. Experimental data is also more reliable at high uranium partial pressure because uncertainties due to self absorption of narrow lines become relatively less important in the presence of increasing continuum activity.

B. Variation of Emissivity with Wavelength

The gross variation of opacity with wavelength, as well as the detailed appearance of the spectrum in any small wavelength region, depends on both the temperature and the uranium partial pressure. In correlating the spectral distribution of energy with the absolute density of uranium, it is reasonable to expect no less scatter than encountered for the absolute emissivity data at 5000 Å. Relative opacity data, however, is very reproducible when normalized against measured absolute emissivity. That is, the relative and absolute photometric variables correlate with each other very well: scatter appears only when one attempts to work back to initial UF_6 concentration. In Figure 17, we placed spectrograms from three experiments onto a common scale of photographic transmissions

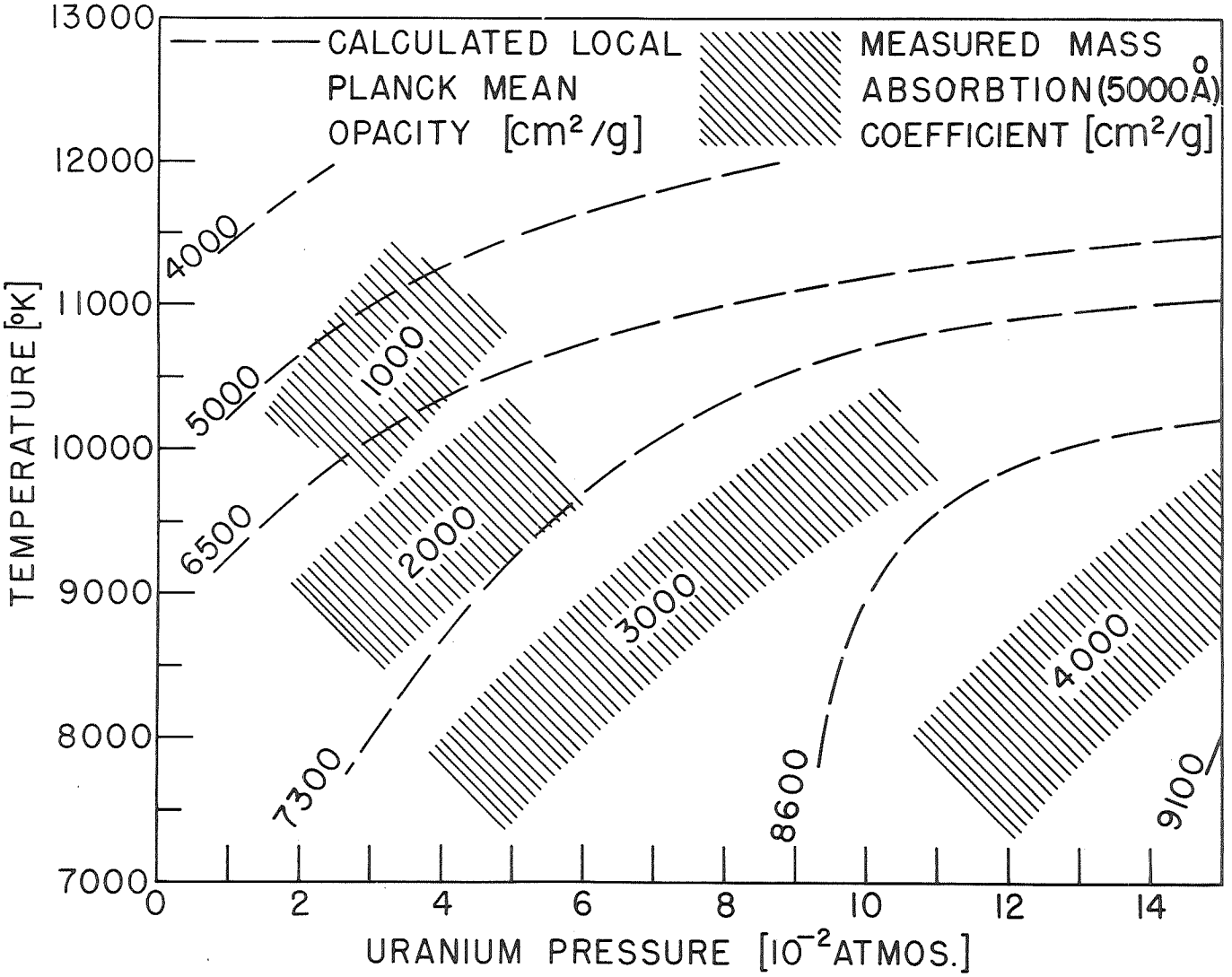

Figure 16. Measured and predicted absolute optical absorption coefficients (5000 Å) for uranium as functions of temperature and uranium pressure. Curves are theoretically predicted contours of constant Planck mean opacity. Shaded areas represent measured mass absorption coefficients.

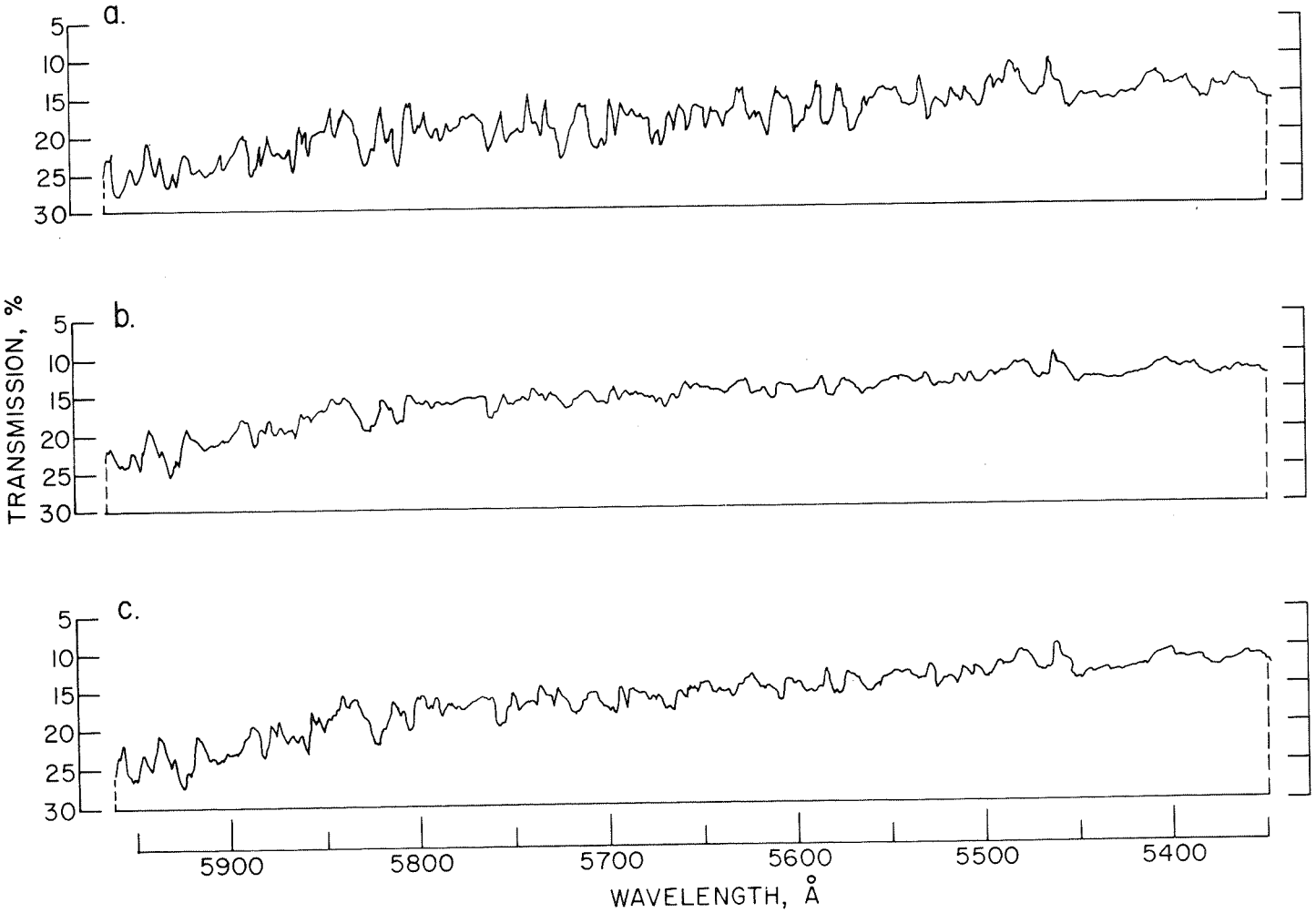

Figure 17. Densitometer tracings (in % transmission) for three shock tube plasmas with similar measured thermodynamic conditions: a.) uranium pressure = 7.7×10^4 d cm^{-2} and T = 8350 °K; b.) uranium pressure = 8.4×10^4 d cm^{-2} and T = 8850 °K; c.) uranium pressure = 8.0×10^4 d cm^{-2} and T = 8500°K. The resolution for these rotating-drum spectrograms is approximately 1.5 Å.

to show how the appearance of the spectrum varies between plasmas having nearly the same measured temperature and uranium partial pressure. The variation of (slit-averaged) optical depth with wavelength and the (apparent) line to continuum ratios do repeat moderately well.

Measured mass absorption for the region 3000-8000 Å is shown in Figure 18. Mean resolution for the data between 3000 and 6800 Å is reduced to 0.3 Å : for the data between 6800-8000 Å , the resolution ia reduced to 1.2 Å because it was necessary to open the spectrograph slits to achieve useful densities on the slower infrared (HSIR) film. The depicted data was obtained from three separate experiments, each covering 1800 Å in wavelength. Tolerance (30%) for wavelengths below 3600 Å are somewhat larger than elsewhere (15-20%), owing to a greater uncertainty in photometric working curves for wavelengths where the sensitivity is inherently low.

The data of Figure 18 have been fitted to theoretical predictions[8] of Planck mean opacity by normalizing the measured absolute mass absorption coefficient at 5000 Å to the calculated values. A most striking feature is the abrupt divergence of theoretical and experimental curves which commences at 4200 Å and grows steadily more pronounced toward lower wavelengths. At 3000 Å the discrepancy in relative opacities has grown to greater than a factor of 10 .

The "bumps" at 4200 Å and 5200 Å are prominent features of the uranium spectra obtained under all shock tube conditions. The density of lines within the 4000 - 4500 Å regions is so great that we cannot discriminate between line and continuum spectra to nearly the extent that was possible at other wavelengths. At this time, we cannot discriminate between two possible origins for these peaks: transitions within favored atomic arrays (particularly UII), or strong ion-continuum interactions.

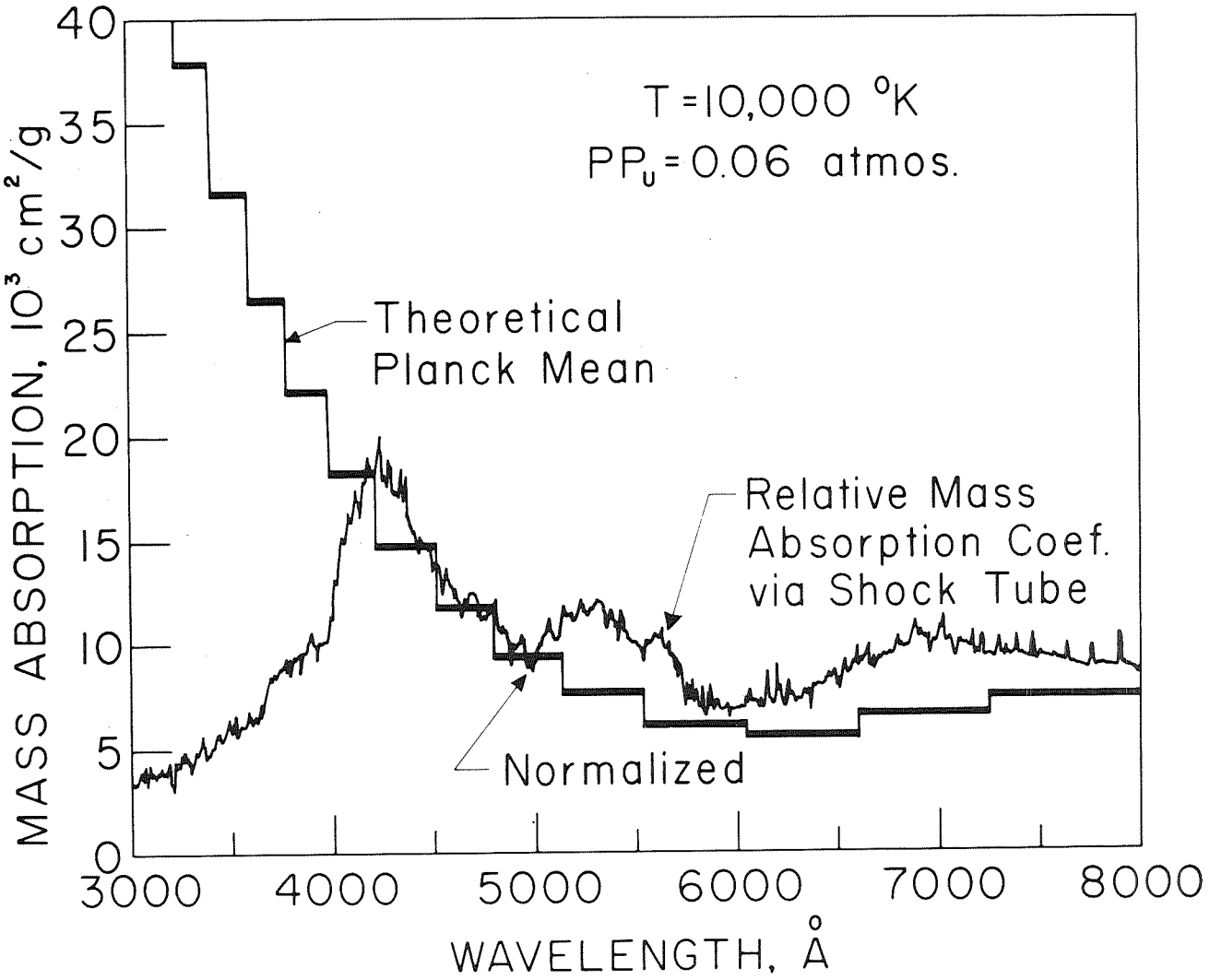

Figure 18. Comparison of experimental and theoretical absorption coefficients (3000-8000 Å) for a plasma temperature of 10,000°K and a uranium partial pressure of 0.06 atmospheres.

The wavelength scale of Figure 18 is too compressed to afford much information on the relation between line and apparent continuum intensities. Therefore, an expanded scale is shown in Figure 19. The depicted spectrum, measured with 0.3 Å slits, is for plasma conditions: $T = 10{,}050°K$, $p = 2.8 \times 10^4$ dcm^{-2}. The computer code[47] which reduces photographic densities to relative intensities, incorporates the aforementioned (Section III F) correction for radiative trapping. The tentative line identification was made with the aid of relative intensity scales in the Handbook of Chemistry and Physics.

C. Work in Progress

Further reduction of the data is continuing in the several areas described below. Pending the outcome of this reduction, results will be selected as subjects of a further report.

More positive separation of line and continuum opacities appears feasible by extensive reduction of the data already obtained. That is, self absorption can be assessed by noting the relative progression of weak and strong (isolated) uranium lines along their respective curves of growth as plasma conditions are changed. This type of reduction is time consuming and is not a fully satisfactory substitute for data obtained directly with the required resolution. Nonetheless, quantitative results are expected because there are numerous pairs of lines whose apparent relative brightnesses differ by a factor of 10 in experiments with low UF_6 concentrations. The relative intensity of such a pair can be followed from shot to shot as the absolute brightness of the weaker line varys by a factor of 5 . It appears doubtful that this method is sensitive enough to also give reliable Stark broadening coefficients, but this is not a prerequisite to determining how well Figure 2 approximates the effect of self absorption upon measured opacity. Once this question is settled, line and (apparent) continuum absorption can be examined separately as

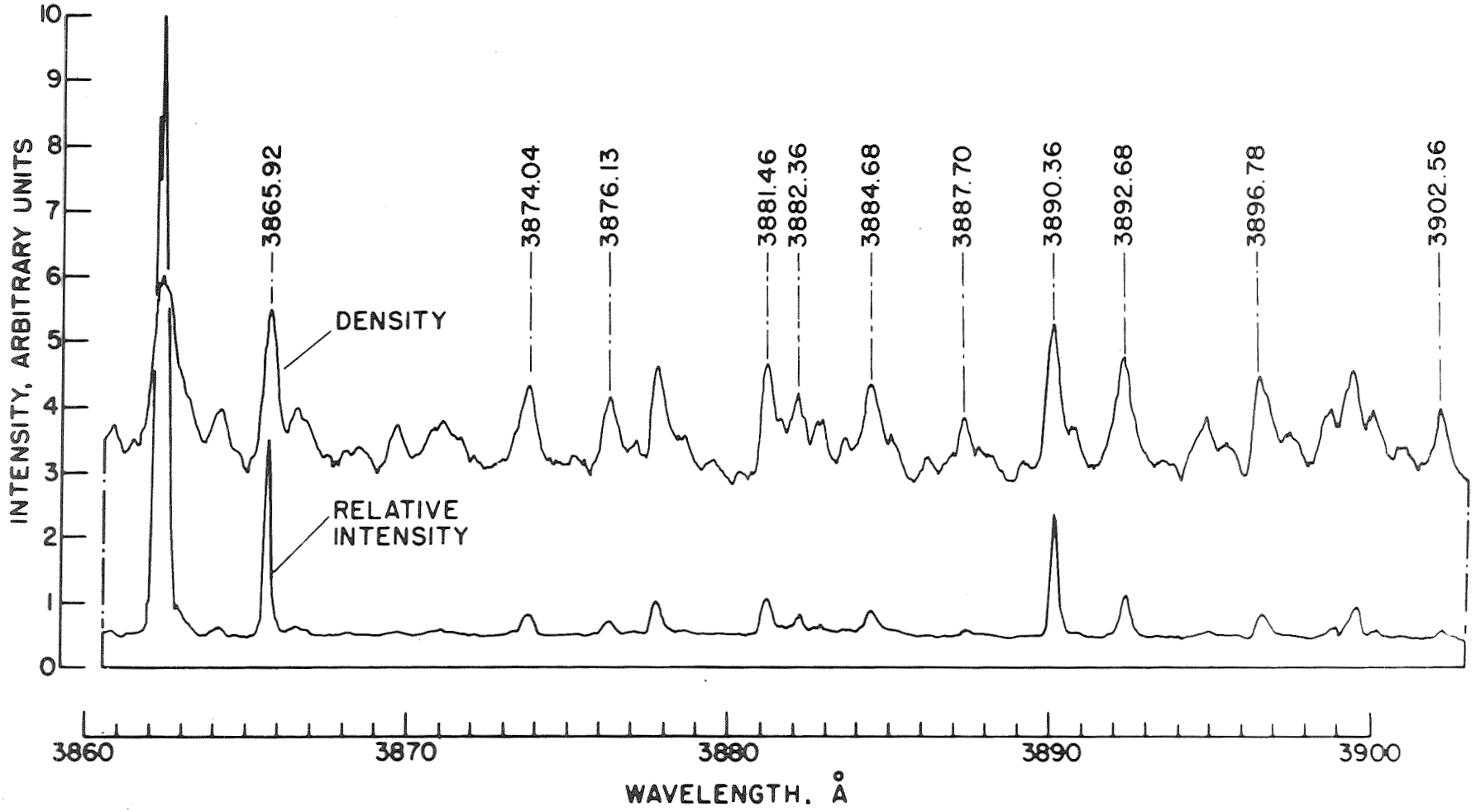

Figure 19. Densitometer tracing (density scale not shown) and corresponding relative intensity record for a portion of a spectrogram having a 0.30 Å resolution. A number of lines can be clearly discriminated from what appears to be the local continuum. None of these profiles has the flat-topped appearance that is characteristic of a saturated spectral line.

functions of T and uranium partial pressure. Moreover, if it proves necessary to apply only moderate corrections for self absorption, there should be no major obstacle to obtaining absolute transition probabilities for some UI lines which are both reliably classified and isolated from other spectral features of comparable strength.

Prospects appear dim that present data can yield more than an upper limit estimate for the Stark broadening of UI lines. Because instrumental profiles are evidently several times broader than the desired Stark halfwidths, statistics from many shots will be required for even a meaningful limit estimate. Currently available films lack the sensitivity that would enable us to use spectrographs of substantially greater dispersion. Accurate, direct broadening measurements may be possible only by using an oscillating Fabry-Perot interferometer in conjunction with a monochromator.[46]

Some hitherto unclassified lines have appeared in the hottest (11,000 - 12,000°K) shocks. The variation of these lines with temperature, and the fact that they have not appeared as persistent impurities in previous shock tube experiments at similar temperatures, suggests that these lines are UIII . Eventually, their wavelengths can be specified to $\pm$ 0.05 Å .

Since it is felt that the mixing methods already used were too rudimentary, a larger mixing chamber with provisions for thorough mixing is now being built. Careful mixing is expected to reduce scatter in the absolute data: if it does not, then the source of nonreproducibility must be sought elsewhere. A mass-spectrometric apparatus of sufficient sensitivity to detect $\sim$ 10 microns of UF_6 in 10 torr of neon would be helpful in this unpleasant eventuality.

A new feature of the observations which is now available is the coverage of a 6000 Å - wide spectral band pass by a single instrument with a $\sim$ 2 Å resolution. This broad coverage makes it much easier to accumulate statistics on the variation of optical depth with wavelength.

By means of UV sensitive plates, the low wavelength cutoff of our measurements will be extended down to 2200 Å, and possibly to 2000 Å. It is important to ascertain whether the predicted UV opacity peaks are, in fact, just the "bumps" already seen in the blue (see Figure 18) or, instead, lie below the 2800 Å cut-off of the data on hand. In any case, it is particularly important to understand the UV region because the Planck function maximum is situated well below 2800 Å at the operating temperatures of proposed gas-core reactors.

V. Conclusions

Absolute optical absorption coefficients of uranium plasmas has been measured for conditions applicable to some regions of proposed gas-core reactors. Uncertainty due to scatter is 40% . The random error is probably generated by unintentional variations (15%) in the amount of UF_6 mixed with neon. No evidence has been found for bias due to decomposition of UF_6 prior to firing the shock tube.

From 4,200 to 8,000 Å, measured absorption coefficients have essentially the same variation with wavelength as theoretically predicted opacities, but are factors of 2 - 5 smaller in absolute value, depending on plasma state. In going from 4200 Å to 2800 Å, however, emissivity is found to steadily decrease, whereas theory predicts a strong <u>increase</u>. This predicted surge in ultraviolet emissivity which leads to a factor-of-10 discrepancy with experiment at 3,000 Å. This might be remedied by

re-evaluating the computer code parameters for low lying levels of UI and UII, or it may require a more basic recasting of the theoretical model. The data indicate that the continuum is responsible for a 5 - 10 times greater fraction of the emissivity than predicted theoretically. It is important that the theory be modified to take satisfactory account of the continuum because Bremsstrahlung emissivities scale roughly with the square of the uranium concentration, while line emissivities have between a linear and a square root dependence. The experiment confirms the theoretical predictions of a negative slope for $\partial K_m/\partial T$. If this were the only consideration, opacities in the center of a gaseous core (temperatures five times greater than this experiment) might amount to only a small fraction of those in the shock tube. However, we also found that the positive slope of $\partial K_m/\partial N_U$ is much greater than estimated by theory. This opposing trend might sustain opacities in the core (where N_U is 10^4-10^5 greater than in the shock tube) at significantly higher levels than heretofore supposed.

ACKNOWLEDGEMENTS

The authors would like to acknowledge the help of D. W. Koopman in providing the high speed computer program for Rankine-Hugoniot calculations. Discussions with R. W. Patch assisted us greatly

REFERENCES

1. F. E. Rom, "Comments on the Feasibility of Developing Gas Core Nuclear Reactors", NASA Tech. Report NASA TM-X 52644 (1969).

2. D. H. Sampson, Radiative Contributions to Energy and Momentum Transport in a Gas, Interscience, New York (1965).

3. S. I. Pai, Radiation Gasdynamics, Springer, Vienna (1966).

4. R. G. Ragsdale and A. F. Kascak, "Simple Equations for Calculating Temperature Distributions in Radiating Gray Gases", NASA Tech. Note TN D-5226 (1969).

5. "MHD Electrical Power Generation - the 1969 Status Report", Joint ENEA/IAEA Laison Group (1969).

6. D. W. Steinhaus, J. Blaise and M. Diringer, "Present Status of the Analysis of the Arc Spectrum of Uranium (UI)", Los Alamos Sci. Rep. LA-3475.

7. B. Osman, thesis, University of Paris (1966). (unpublished).

8. D. E. Parks, G. Lane, J. C. Stewart and S. Peyton, "Optical Constants of Uranium Plasmas", NASA Tech. Report NASA CR-72348 (1968).

9. C. W. Allen, Mon. Not. R. Astr. Soc. 133, 21 (1966).

10. J. N. Bradley, Shock Waves in Chemistry and Physics, Methuen, London (1962).

11. T. D. Wilkerson, "The use of the Shock Tube on a Spectroscopic Source with an Application to the Measurement of gf-Values of Cr I and Cr II", Thesis, Michigan (1961).

12. J. K. Wright, Shock Tubes, Methuen, London (1961).

13. Y. B. Zel'dovich and Y. P. Raizer, Physics of Shock Waves and High-Temperature Hydrodynamic Phenomena, Academic Press, New York (1966).

14. T. D. Wilkerson, D. W. Koopman, M. H. Miller, R. D. Bengtson and G. Charatis, Phys. Fluids Supplement 1, I-22 (1969).

15. A. G. Gaydon and I. R. Hurle, The Shock Tube in High Temperature Chemical Physics, Chapman Hall, London (1963).

16. Parkinson, W. H., and Nicholls, R. W., Shock Tube Spectroscopy III: Temperature and Intensity Measurements in a Shock Tube, U. of Western Ont. Phys. Dept. Report, AFCRC-TN-59-662 (1959).

17. P. W. J. M. Boumans, Theory of Spectrochemical Excitation, Plenum New York (1966).

18. J.M. Bridges and W. L. Wiese, Phys. Rev. 159, 31 (1967).

19. H. R. Griem, Plasma Spectroscopy, McGraw-Hill, New York (1964).

20. J. Richter, Chapter 1 in Plasma Diagnostics (ed. W. Lochte-Holtgreven), Wiley Interscience, Amsterdam (1969).

21. D. Robinson and P. Lenn, Appl. Opt. 6, 893 (1967).

22. E. W. Foster, Rep. Prog. Phys. 27, 469 (1964).

23. A. T. Hattenburg, Appl. Opt. 6, 95 (1967).

24. W.R.S. Garton, W. H. Parkinson and E. M. Reeves, Proc. Phys. Soc. 88, 771 (1966).

25. W.R.S. Garton, J. Sci. Instr. 30, 119 (1953).

26. M. H. Miller and R. D. Bengtson, "A New Method of Absolute Intensity Calibration", JQSRT 9, 1573 (1969).

27. R. W. Patch, JQSRT 7, 611 (1966).

28. J. T. Davies and J. M. Vaughan, Ap. J. 137, 1302 (1963).

29. W. L. Wiese, Chapter 6 in Plasma Diagnostic Techniques, (ed. R. H. Huddlestone and S. L. Leonard), Academic Press, New York (1965).

30. J. Cooper and G. K. Oertel, Phys. Rev. 180, 286 (1969).

31. S. Sahal - Brèchot, Astron. Astrophysics. 1, 91 (1969); 2, 332 (1969).

32. M.H. Miller, "Thermally Insensitive Determinations of Transition Probabilities for CI, OI, NeI, AlII, SiI, SiII, PI, PII, SI, SII and ClI, University of Maryland, Tech. Note BN-550 (1968).

33. R.D. Bengtson, "The Measurement of Transition Probabilities and Stark Widths for CI, FI, NeI, ClI, ClII, BrI and BrII, University of Maryland, Tech. Note BN-559 (1968).

34. R.D. Bengtson, M.H. Miller, D.W. Koopman, and T.D. Wilkerson, Phys. Fluids 13, 372 (1970).

35. M.H. Miller, JQSRT 9, 1251 (1969).

36. S.M. Wood and M.H. Miller, "A High Speed Spectrograph Shutter", NASA Tech. Report NASA CR-72660 (1970).

37. J.W. Arendt, E.W. Powell and H.W. Saylor, "A Brief Guide to UF_6 Handling", AEC Report TID-4500 (1956).

38. P.L. Byard and R.E. Roll, JQSRT 5, 715 (1965).

39. E.M. Carnevale, S. Wolnik, G. Larson, C. Carey and G.W. Wares, Phys. Fluids 10, 1459 (1967).

40. P. Kepple and H.R. Griem, Phys. Rev. 173, 317 (1968).

41. M.H. Miller and R.D. Bengtson, "Measured Stark Widths and Shifts for Neutral Atomic Lines", Phys. Rev. (in press for April 1970).

42. R.D. Bengtson, M.H. Miller, W.D. Davis and J.R. Grieg, Ap. J. 157 957 (1969).

43. W.L. Wiese, M.W. Smith and B.M. Glennon, Atomic Transition Probabilities, Vol. I: Hydrogen through Neon, Nat. Bur. St. Ref. Sev. 4 (1966).

44. R.D. Bengtson and M.H. Miller, "Experimental Transition Probabilities for Neon I," J. Opt. Soc. Am. (in press).

45. T.D. Wilkerson, pps. 487-503 in Dynamics of Fluids and Plasmas, Academic Press, New York (1966).

46. J. Cooper and J.R. Grieg, J. Sci. Instrum. 40, 433 (1963).

47. R.A. Bell, R.D. Bengtson, D.R. Branch, D.M. Gottlieb, and R. Roig, "Computer Programs for Reduction of Microphotometer Data", University of Maryland, Tech. Note BN-572 (1968).